POLITECNICO DI TORINO

Master of Science in Biomedical Engineering

Master's Degree Thesis

Muscle synergy extraction during gait and cycling: effect of EMG detection at different locations along bi-articular muscles

Supervisors:

Marco Gazzoni

Taian Martins Vieira

Giacinto Luigi Cerone

Candidate:

Alice Chiara Moretti

December 2021

Abstract

Muscle synergies represent a model of how the Central Nervous System (CNS) recruits different muscles, coordinating their activation during a functional task. Muscle synergies are usually estimated from surface EMG signals, recorded with bipolar technique, from the group of muscles involved in the movement under study; usually, one bipolar detection system per muscle is used. However, studies in the literature have suggested that some lower limb muscles (Rectus Femoris, Gastrocnemius Medialis, Vastus Medialis, Soleus) are not uniformly activated during a motor task, but separated regions are selectively recruited in different phases of the movement.

This study aims to evaluate if muscle synergies extracted during gait and cycling depend on the electrode position on the muscle. High-density EMG technique has been used to simulate different electrode positioning.

Eight healthy male subjects were recruited for this study. EMG signals were detected from Rectus Femoris, Gastrocnemius Medialis, Vastus Medialis, Vastus Lateralis, Soleus, Biceps Femoris, Gluteus Medius, and Tibialis Anterior during i) over ground gait at a natural pace and ii) during cycling without pedal-straps. HD-sEMG was recorded from Rectus Femoris and Gastrocnemius Medialis muscles to distinguish proximal and distal muscle regions. Movement kinematics was recorded using a 12-camera optoelectronic system.

The HD-sEMG signals recorded from Rectus Femoris and Gastrocnemius Medialis were used to simulate three bipolar detection systems for each muscle: one matching the SENIAM recommendation, one proximal, and one distal. Muscle synergies were extracted considering all possible combinations of real and simulated signals. The extraction of synergies was performed using Non-Negative Matrix Factorization.

In general, the extracted synergies were repeatable and consistent with the literature. During the gait task, in 1 out of 5 subjects, the coefficients of the synergy where Rectus Femoris mainly participates, show a peak between the 60% and the 80% of the gait cycle corresponding to the middle of the swing phase. The peak amplitude decreases moving from the proximal to the distal electrode positioning. This result highlights some degree of variability in RF muscle activation during gait with, in some cases, the localized regional activation of Rectus Femoris for hip flexion and knee extension. The synergy where Gastrocnemius Medialis is mainly represented does not show an electrode positioning dependent behaviour.

During the cycling task, the coefficients of the synergy where Rectus Femoris knee extension function is mainly represented show increasing values moving from proximal to distal electrode positioning during downstroke phase, while the synergy where Rectus Femoris hip flexion function is mainly represented show decreasing coefficient values moving from proximal and distal region during upstroke phase where hip flexion occurs.

The two synergies where Gastrocnemius Medialis is mainly represented corresponding to plantar flexion during the downstroke phase, and knee flexion during upstroke phase do not show significant differences moving from proximal to distal electrode positioning.

The results show that in some cases synergies are affected by electrode positioning. Due to the low number of subjects included in this work it is not possible to generalize the results, but further studies are probably needed to understand the real impact of these preliminary observations.

Acknowledgements

I would like to thank all LISIN staff members who helped me throughout the duration of this work, in particular Professor and LISIN director M. Gazzoni, Prof. T. Vieira Martins and G. L. Cerone.

My parents Massimo and Paola who have always supported me throughout my university career.

Thanks to my love Edoardo and my friends who have always been close to me at difficult times.

Special thanks to my beloved grandfather Cesare, who cannot be here to share this immense joy, but always believed in me.

To my family

Index

List of Figure

1 Introduction

Muscle synergies are investigated with attention by modern research. They provide knowledge on how Central Nervous System (CNS) recruits certain muscles, by combining their activation during specific phase of a motor task to simplify movement production. However, specific studies [20][21][22][24] have shown that some biarticular muscles don't activate uniformly, but certain portions seem to be more involved at specific phase of a task than others. This has led to the hypothesis that muscle synergies could vary if different muscle regions are considered as independent actuators.

Moreover, fibers' configuration and pennation angle is a very important variable when we must place electrodes correctly, in addition, Saitou et al. [32] have documented that some muscles mentioned don't have a region where the innervation zone is localized, but it is scattered or distributed in complex configuration.

In this study, the focus is on biarticular muscle that show different activation level during a specific task, as documented in literature. Rectus Femoris and Gastrocnemius Medialis were the muscles chosen for this investigation. Usually when synergy extraction is performed, one couple of electrodes is placed on each muscle, following SENIAM recommendation for electrode positioning. The aim of this work is to verify if changing electrode placement along these muscles lead to difference on muscle synergies. First, it is important compare muscle synergies with those finding in literature, to check algorithm stability; Barroso et al. [17] was the reference article, because they performed synergy extraction during both walking and cycling.

Muscle synergy extraction was performed on MATLAB 2018b® with MATLAB NNMF routine (non-negative matrix factorization), while pre, post-processing and results visualization was performed using MATLAB customized scripts. Muscle synergies was firstly compared for each subject to check if a different positioning has led to evident difference and the repeatability among all subject was checked. Muscle synergy weights is the most important variables for the comparison because they show the activation level of each muscle in a synergy, activation coefficient could show some difference too, but it's more difficult to assess due to the EMG variability.

2 EMG signal and concepts of electromyography

2.1 Generation of EMG signal

EMG signal provides us with information about the strategies that the CNS adopts to generate a voluntary movement, therefore it is essential a description of the human neuromuscular system to understand how muscle generate bioelectrical signals.

The basic unit of the neuromuscular system is called motor unit (Fig. 2.1 A), it comprises a motor neuron and the muscle fibers innervated by his axon, thus an action potential generated by the motor neuron results in an activation of the innervated muscle fibers (Fig. 2.1B). The cell membrane resting potential is about 70 mV, negative inside the cell, this is possible thanks to the sodium-potassium pump, that works against the concentration gradient of the ions. When the action potential reaches the point where the axon end-plate innervates the muscle fibers, known as neuromuscular junction, acetylcholine is released (Fig. 2.2). This is a neurotransmitter that binding with specific receptors causes the opening of ions channels, so the sodium can flow inside the membrane causing the depolarization of the cell membrane and the generation of an action potential. The action potential propagates along the fiber from the innervation zone to the tendons, where the potential dies out.

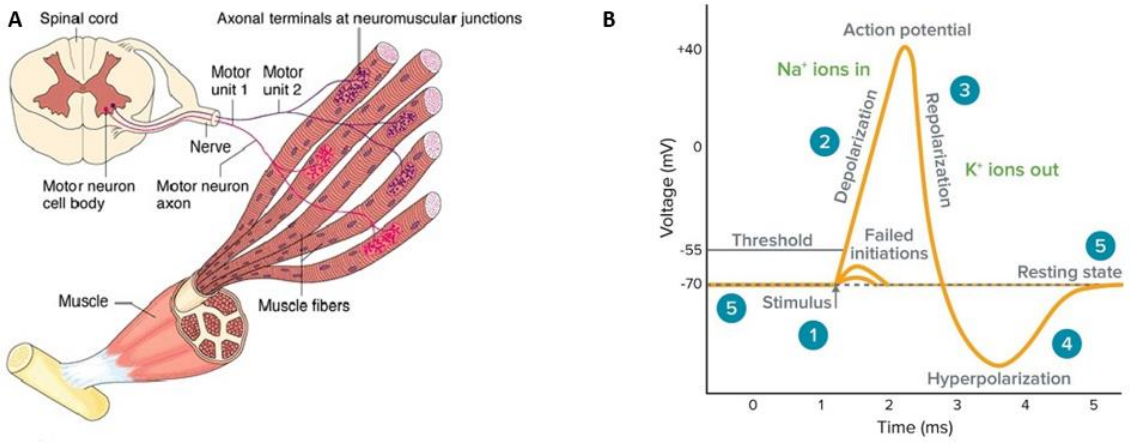

Figure 2.1: : (**A**) a schematic representation of the motor unit structure. (**B)** shape of the muscle fibers' action potential: the release of acetylcholine causes the depolarisation of the membrane with an in-flux of Na^+ ions, then a repolarization phase occurs, with an out-flux of K^+ ions. At last, the muscle fibers enters in a refractory period (hyperpolarization phase).

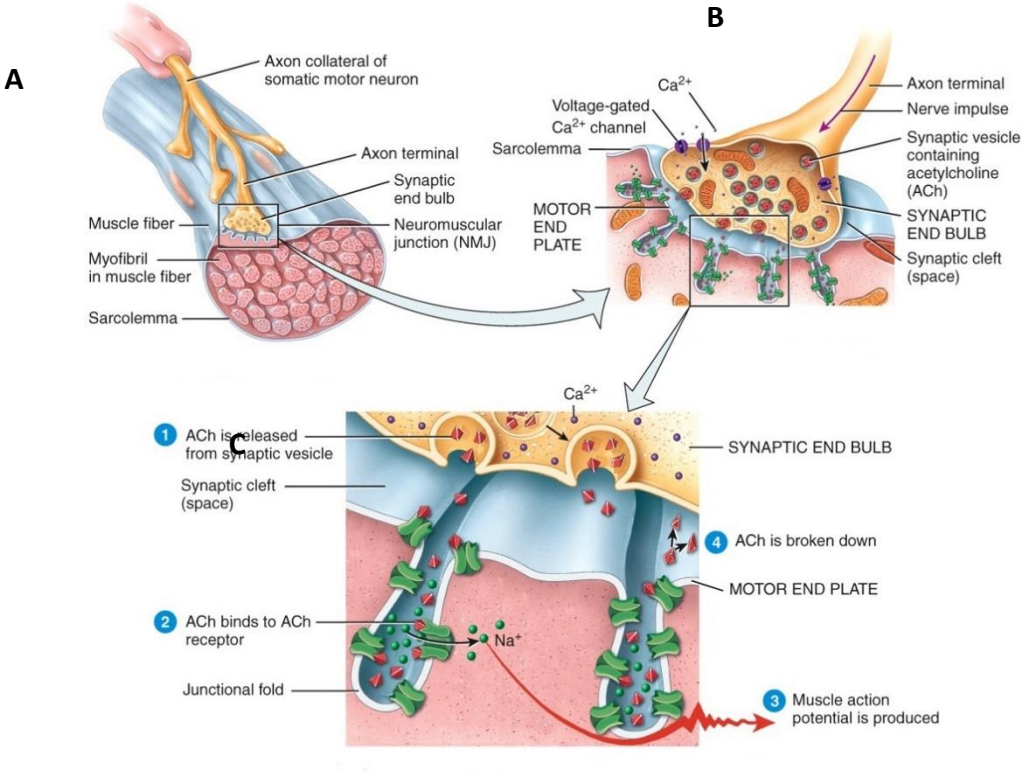

Figure 2.2: (**A**) architecture of a muscle fiber. (**B**) enlarged view of a neuromuscular junction. (**C**) Binding of acetylcholine to ACh receptors in the motor end-plate.

To represent the current distribution into the depolarization zone of the muscle fiber the triplets of charges model is used, its main characteristic is the fact that the total charge intensity is null, because of there is two negative and one positive charge that compensate each other when they reach the tendons, this process is detected under the electrodes as a high-intensity common mode effect, known as 'end-of-fiber-effect' (Fig. 2.3).

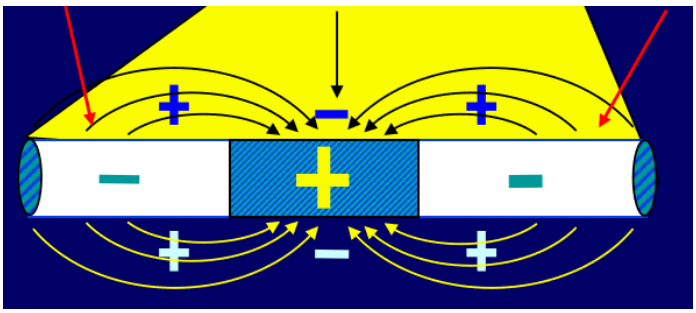

Figure 2.3: representation of the myoelectric potentials as a triplet of charges model.

2.2 Introduction to surface EMG

The most used technique to detect EMG signal in research and clinical environments is based on surface electrodes made of Ag or Ag-Cl simply positioned on the subject's skin. The action potential, as said earlier, propagates from the motoneuron to muscle fibers causing their depolarization and contraction; this potential is called MUAP (motor unit action potential). Surface EMG (sEMG) is a combination of all potentials coming from all the fibers contained in the acquisition volume defined by the interelectrode distance (IED), the result is an interference signal (Fug. 2.4).

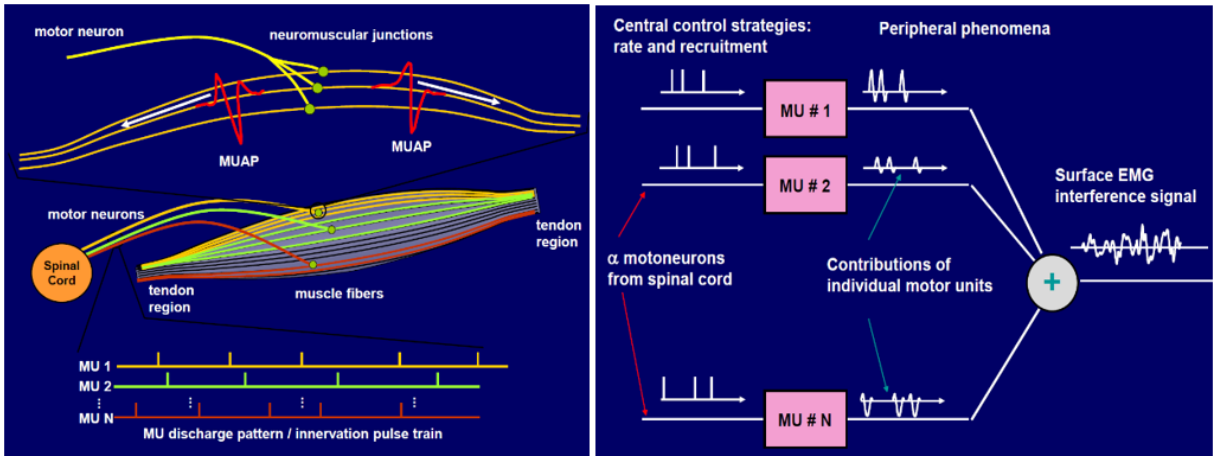

Figure 2.4: (**A**) a schematic representation of how the potential propagates from motoneuron to neuromuscular junction, where MUAP generates, and it propagates along the fiber. (**B**) MUAP summation during voluntary contraction.

Interelectrode distance is a fundamental parameter for sEMG detection, because the higher IED, the larger acquisition volume is and more muscle fibers' going to be contained in the volume, so the resulting signal is more representative of the muscle activity. A too much high interelectrode distance could cause 'crosstalk', that is when acquisition volume includes fibers which belong to a nearby muscle; it must be avoided to perform a correct sEMG acquisition (Fig.2.5).

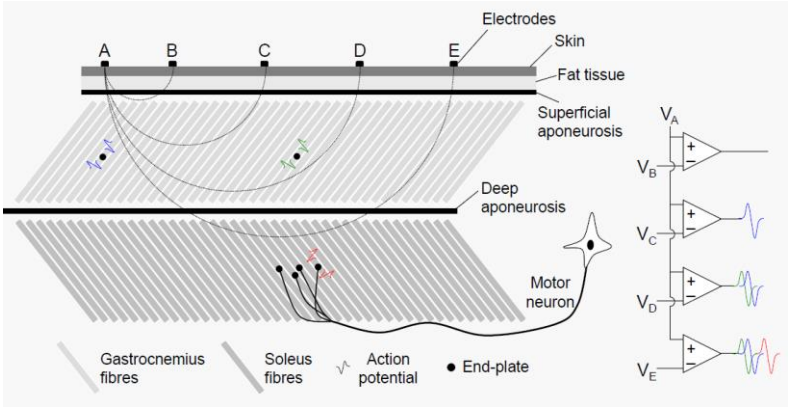

Figure 2.5: influence of different interelectrode distances on acquisition volume as it can see a higher distance can cause crosstalk, because the soleus fibres activity is detected

Another aspect is skin preparation. The electrode-skin interface is a source of noise, for this reason is important to clean, scrub the skin under the electrodes and hair must be removed to guarantee a high-quality electrode-skin interface.

In any case, subcutaneous tissue has a low-pass filter effect on the signal, in fact an increasing of thickness results in a decreasing of the amplitude of the signal and the signal bandwidth is reduced. Even the pennation angle influences the signal features, but it's difficult to predict it, because it depends on the interelectrode distance, the electrodes size and shape (Fig. 2.6).

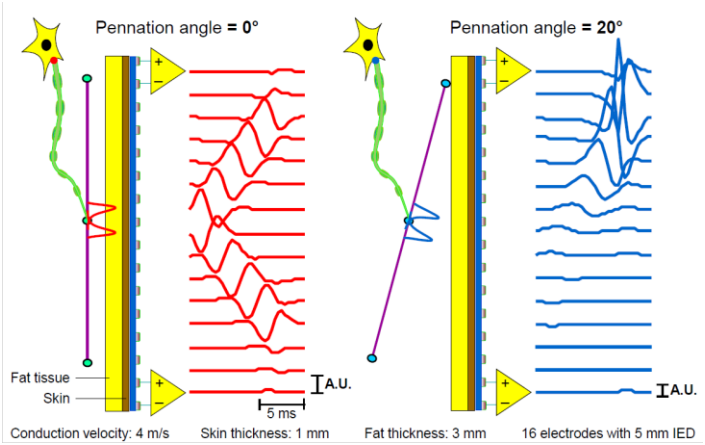

Figure 2.6: : a non-null pennation angle can critically affect the representation of action potential s in surface EMG, because the distance from the source change along the fibre length.

2.3 Surface EMG electrode configuration

sEMG can be detected by means of different electrodes configurations (Fig. 2.7):

- Monopolar configuration (MP): there is a detecting electrode and a reference electrode, is used only in research because of its sensitivity to common-mode signals.
- Single-differential configuration (SD): is the most used configuration, signals are detected from two active electrodes, and the output is the difference between the two detected signals. Bipolar acquisition can be done with many couple of electrodes, obtaining N-1 SD signals, from N electrodes. This configuration solves the problem of monopolar because it can filter most of the common mode and makes the propagation of the potential along the muscle more evident.
- Double-differential configuration (DD): signals will be the difference between two SD signal, is useful to reduce the crosstalk, because limit the acquisition volume, estimate conduction velocity, and increase the selectivity.

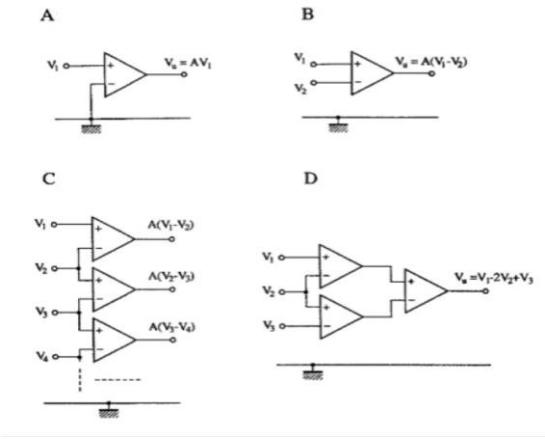

Figure 2.7: different electrode configuration for sEMG detection: (**A**) monopolar configuration, (**B**) single-differential, (**C**) cascade of single-differential and (**D**) double-differential.

Using a single couple of electrodes can be insufficient to represent the total muscle activity, so most advanced techniques are developed. These are based on multichannel detection using one- or two-dimensions electrode arrays and are known as high-density EMG (HD-sEMG) through which a spatial map of EMG distribution in a muscle can be obtained (Fig. 2.8).

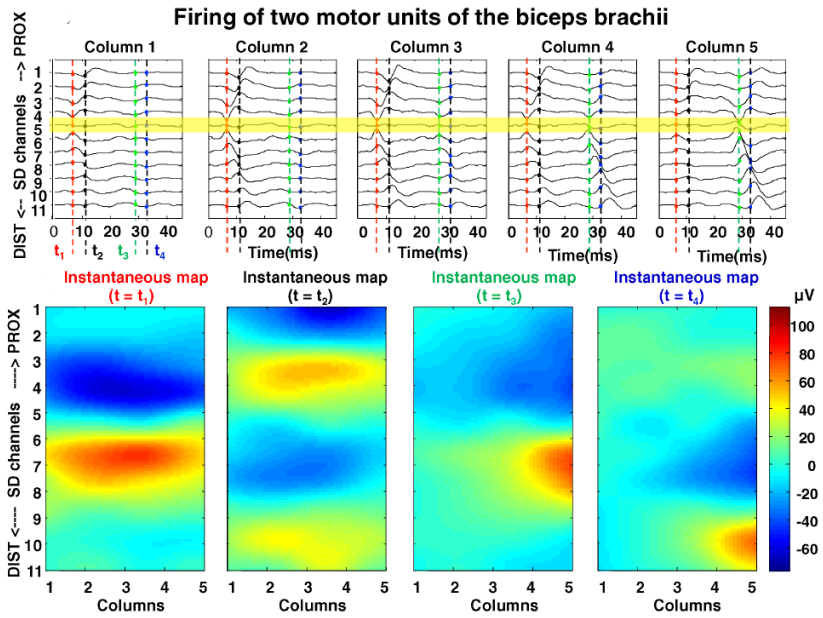

Figure 2.8: 2-D electrode array with 12 rows and 5 columns and five sets of single SD signals, each set obtained from one column. The electrode grid is placed on a biceps brachii, during a mild voluntary isometric contraction, with columns parallel to the fiber direction.

3 Muscle Synergy Extraction

3.1 Introduction on muscle synergies

Many researchers since Bernstein (1967) have acknowledged that when the CNS generates voluntary movement a certain set of muscles are simultaneously activated and coordinated. This discovery has led to the hypothesis that the motor system manages a large set of movement combining motor modules, known as muscle synergies [1]. Understanding how CNS generates movement is difficult because of the redundancy of the neuromuscular system, for this reason muscle synergies can be conceived as 'building blocks' that can simplify the reconstruction of motor control and reduce the degrees of freedom [2][3].

Therefore, muscle synergies are strategies that the CNS adopts to recruit different muscles, coordinating their activation to perform a certain task; each has its set of muscle synergies and activation patterns of their muscle, but there is evidence that some basic muscle synergies are shared across different motor task [4][5].

Another important consideration is the clinical assessment. Muscle synergies, as said before, are motor modules that describe neural control of limbs movements, for these reasons they can be used as a tool for assessment of neuromotor disease (stroke patients) and the motor recovery after rehabilitation treatment, combining, for example, synergies and biomechanical analysis [6][7].

3.2 Mathematical models of muscle synergies

In literature two models for muscle synergies are proposed: time-invariant (or synchronous) and time-varying (or asynchronous) models [8][9][10].

In the first model the control input u(t) is a linear combination of k vectors w, that is a scalar synchronous value, multiplied by time-varying coefficient a, k represents the number of synergies.

$$u(t) = \sum_{j=1}^{k} a_j\,(t) w_j$$

In other words, vectors *u* represents a balance between muscle activation, and its coefficient *w(t)* determines its temporal evolution.

On the other hand, in the time-varying model synergies are asynchronous, this means that each vectors w, that represents synergies weight, can be scaled, and shifted in time by a and τ (Fig. 3.1).

$$u(t) = \sum_{j=1}^{k} a_j \, w_j(t - \tau_j)$$

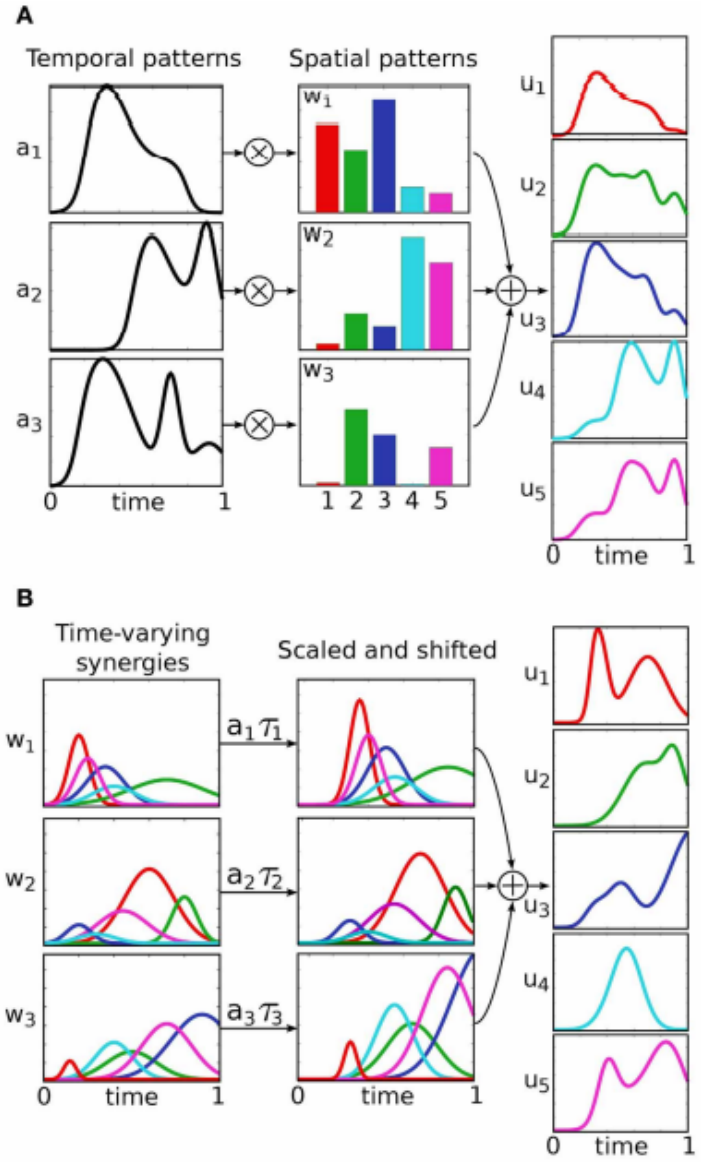

Figure 3.1: Cristiano et al. [9] **(A)** Time invariant model, temporal patterns represent the activation levels of all muscles combined during the task, and the spatial patterns (or weights) specifies how much a muscle is active for that specific. Temporal pattern, in this model temporal and spatial pattern are linearly combined. **(B)** Time-varying model, in this case vectors w represents both temporal and spatial information, and they are scaled and shifted in time to map the entire muscle activities.

In this work time-invariant model for muscle synergies has been chosen in accordance with the choice of factorization algorithm and the previous study in literature [9][10].

3.3 Matrix factorization techniques: NNMF algorithm

In literature many factorization algorithms for extracting muscle synergies have been proposed and their performance have been confronted [11][12][13], in particular principal component analysis (PCA), which performance is lower the other algorithms, factor analysis (FA), independent component analysis, that works well on data sets with corrupted by constant variance Gaussian noise and nonnegative matrix factorization (NNMF), that performs very well on data sets with signal-dependent noise [11]. This algorithm, moreover, is the most used in literature [10] because is readily available in many data processing packages, like MATLAB, for these reasons it has been chosen in this thesis for muscle synergies extraction.

The NNMF algorithm takes as input sEMG matrix, with dimension m x t, where m indicates the number of analysed muscles, then t is the duration of signal, expressed as number of samples. This algorithm extracts r synchronous muscle synergies, by dividing the initial matrix in 2 sub-matrixes as below (Fig. 3.2)

- Spatial pattern, indicated by W, or weights provide information about the level of activation of the single muscle for each synergy and has dimension m x r where r is the number of synergies.

- Temporal pattern, indicated by H, or muscle synergies activation matrix consist of time-varying synergies activation profile and has dimensions r x t.

- sEMGr is the reconstructed EMG matrix and it's obtained by multiplication W*H, but it isn't the same of the initial one but contains a residual error.

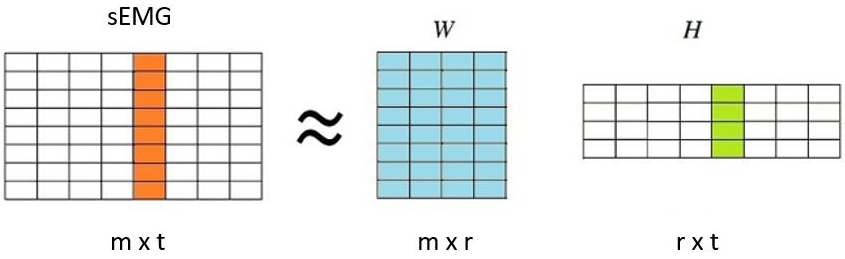

$$sEMGr = \sum_{j=1}^{r} w_j h_j(t)$$

$$sEMG = \sum_{j=1}^{r} w_j h_j(t) + e$$

$$sEMG \approx W\ x\ H(t)$$

Figure 3.2: simple representation of the sEMG signal, which is devided into W (sinergies' weights matrix) and H (activation coefficient matrix).

Number of extracted synergies, as already said, has to be declared before NMF inizialization. To selected the correct numeber of muscle synergies a parameter called variance accounted for (VAF), which indicates how small the factorization error is and how accurate the reconstruction of the original signal was (Fig. 3.3).

$$VAF(\%) = \left[1 - \frac{(EMG_0 - EMG_r)^2}{EMG_0^2}\right] * 100$$

Where EMG_0 is the original signal and EMG_r is the reconstucted one.

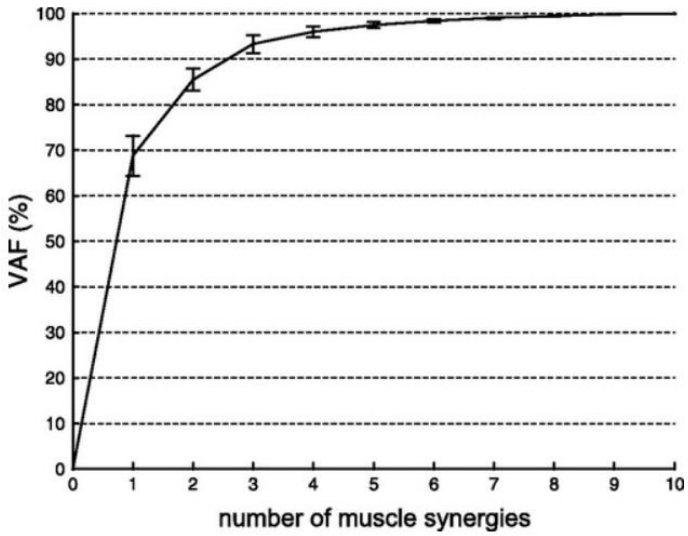

Figure 3.3: VAF trend as a function of the number of extracted synergies.

As seen in figure 3.3, VAF varies from 0 to 1 (in percentage in the figure), and a higher number of synergies lead to a higher VAF value, so better the reconstruction will be. It is, however, unnecessary a VAF with value 1, in literature [14][15] a VAF of 90% or 95% is enough to reconstruct the EMG signal, so the number of synergies will be the one in correspondence of this VAF value.
VAF can be also calculated for each muscle signal and a cut-off value set at 75% were used to consider the reconstruction of the signal acceptable [16][17].

3.4 Muscle synergies during gait and cycling: previous studies in literature

There are several examples in the literature of studies about muscle synergies extraction during gait and cycling, which investigate their main characteristics.

Commonly four to seven synergies are found as regards gait analysis (Barroso et al. [17], Kibushi et al. [16], Cappellini et al. [13] and Rimini et al. [18]).

Referring to the Barroso's work, four synergies come out (Fig. 3.4):

- The first synergy is characterized by the activity of Gluteus Medius, that is a hip flexor and hip abductor, and the Tibialis Anterior, ankle dorsiflexor. This synergy is also

marked by the activation of the Vastus Lateralis for high speed and is mainly activated during stance phase.

- The second synergy reveals two peaks, one at midstance phase and the other at the beginning of the swing phase. These peaks represent the activation of Rectus Femoris, hip flexor and knee extensor, Vastus Lateralis and Tibialis anterior.
- The third synergy is activated at late stance, and it is characterized by the activation pf Gastrocnemius Medialis, knee flexor and ankle plantar flexor, and SOL, ankle plantar flexor.
- The fourth synergy is represented by the activation of Biceps Femoris, hip extensor and knee flexor, Semitendinosus, hip extensor, and knee flexor, and Tibialis Anterior at terminal swing and initial stance phase.

By increasing the number of synergies it is possible to give further details of the muscle activation and the quality of the reconstruction of the original signal increase, but they don't provide with any new information about the neural motor control.

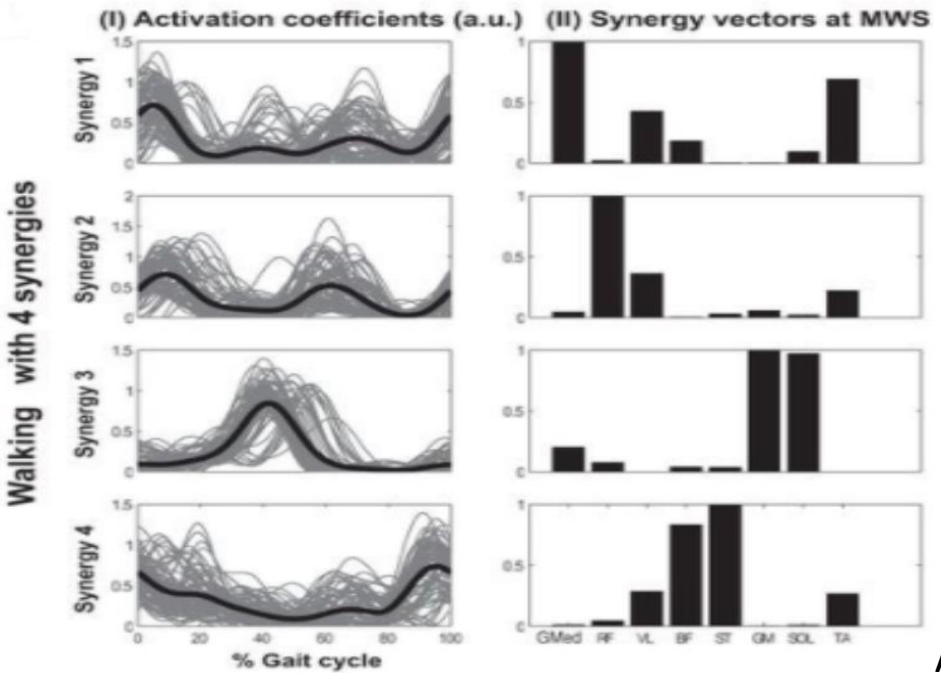

A

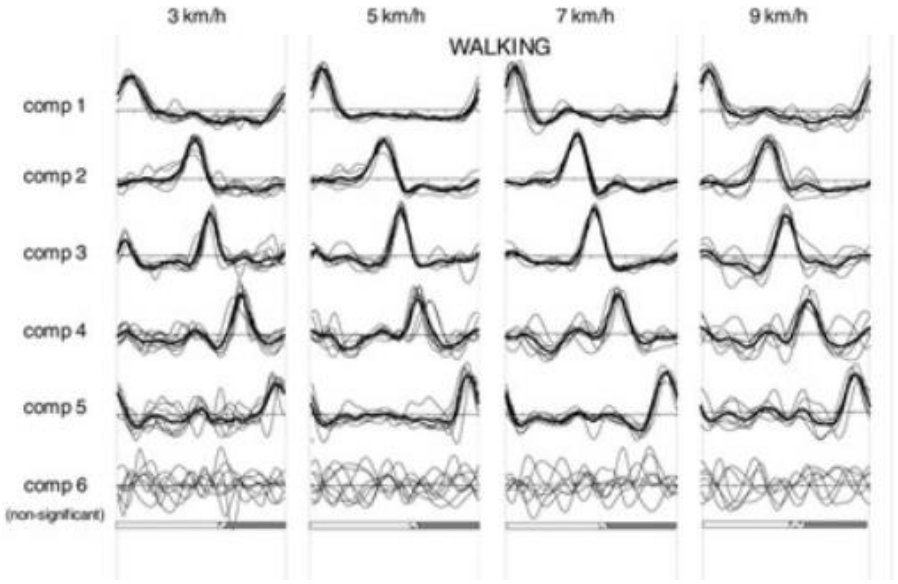

B

Figure 3.4: **A)** Barroso et al. [17] work about muscle synergies extraction during gait. To extract the synergies they used NMF algorithm concatenating the EMG envelopes of ten consecutive walking cycles. Synergies 1 and 2 describes stance phase; synergies 3 and 4 describe swing phase. Gray lines represent activation coefficient of all subjects ten cycles, and black line is the average of the cycles. Analysed muscles are: GMed (Gluteus Medius), RF (Rectus Femoris), VL (Vastus Lateralis), BF (Biceps Femoris), ST (Semitendinosus), GM (Gastrocnemius Medialis), SOL (Soleus), TA (Tibialis Anterior). **B)** Cappellini et al. [13] activation coefficient during walking at different speed, different factorization algorithms are performed using 32 muscles and concatenating more than 10 cycles.

Typically, three synergies are enough to reconstruct EMG signal during cycling with high quality (Barroso et al. [17], see Fig 3.5, and Hug et al. [19]).

- The first synergy is represented by the activation of Tibialis Anterior, Rectus Femoris, Gluteus Medius and Soleus during upstroke phase of cycling.
- The second synergy describes the activity of Rectus Femoris, Gluteus Medius, Vastus Lateralis and Soleus during final upstroke phase and initial downstroke phase.
- The third synergy is characterized by activation of Biceps Femoris, Semitendinosus, Gastrocnemius Medialis and Soleus during the downstroke phase.

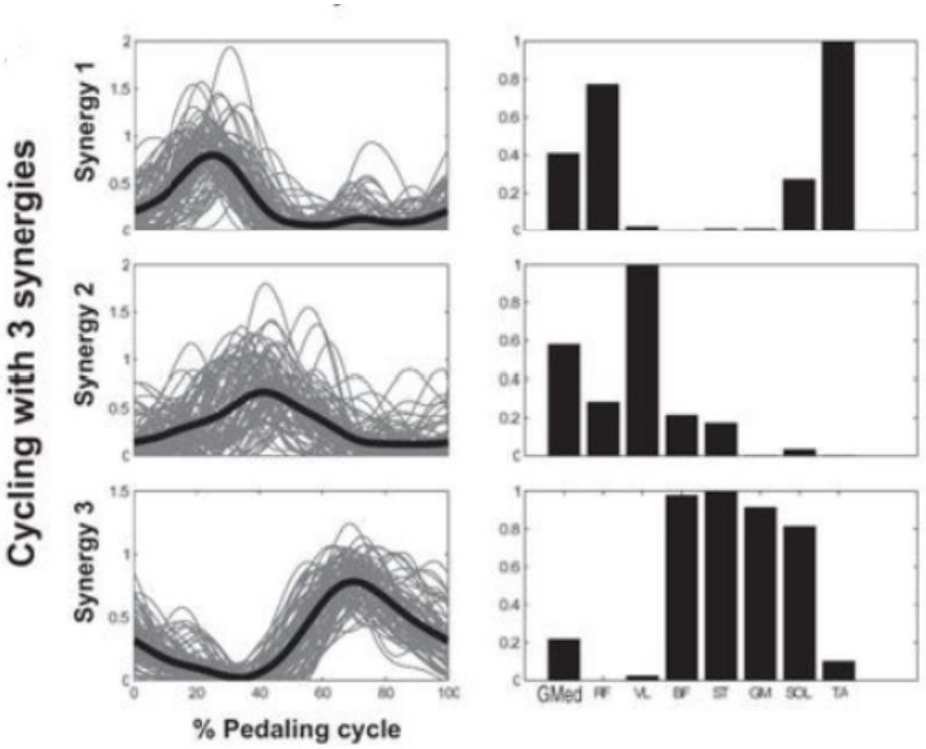

Figure 3.5: Barroso et al. [17] study of muscle synergies during cycling. To extract the synergies they used NMF algorithm concatenating the EMG envelopes of ten consecutive bike cycles. Synergies 1 and 2 describe upstroke phase and the beginning of downstroke phase; synergy, 3 is referred to downstroke phase. Gray lines represent activation coefficient of all subjects ten cycles, and black line is the average of the cycles. Analysed muscles are: GMed (Gluteus Medius), RF (Rectus Femoris), VL (Vastus Lateralis), BF (Biceps Femoris), ST (Semitendinosus), GM (Gastrocnemius Medialis), SOL (Soleus), TA (Tibialis Anterior).

3.5 Rationale for the study and state of art

In literature there is evidence that shows how some muscles show a different behaviour from proximal to distal regions, i.e., Rectus Femoris, Gastrocnemius Medialis and Vastus Medialis, and from medial to lateral regions, as regards Soleus.

- Rectus Femoris is a hip flexor and a knee extensor. Figure 3.6 from Watanabe et al.[22] shows that Rectus Femoris' proximal and distal region are independently activated during different task task. In Watanabe et al. [20] spatial distribution of the activation pattern of this is analysed during gait on a treadmill at different speeds and gradients, suggesting that this muscle is non-uniformly activated during a gait cycle. First, they calculated root mean square (RMS) values of surface EMG and then they averaged this value every 2% of a stride across 20 strides, finally they averaged all results among all subjects and gait condition. As it can see from figure 3.7 during heel contact (20-90% of gait cycle), corresponding to knee extension, distal region

of Rectus Femoris is mainly activated, on the other hand at toe-off (approximately 60% of gait cycle), corresponding to hip flexion, proximal region is majorly involved.

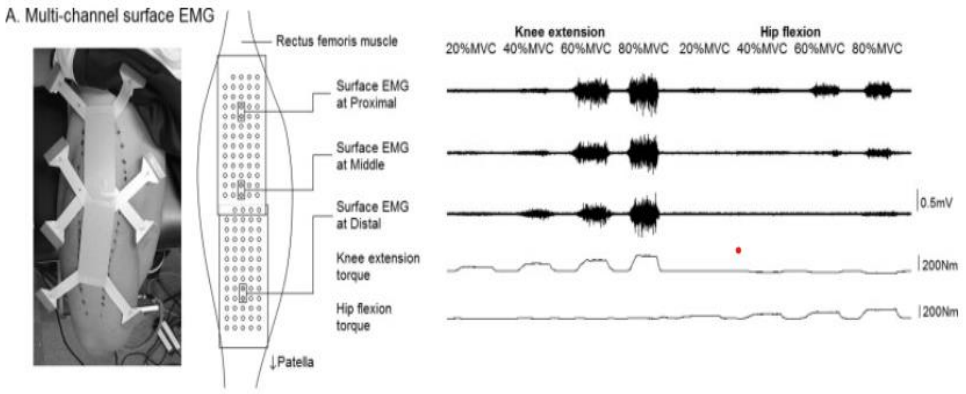

Figure 3.6: (picture from Watanabe et al. [21]): Watanabe et al. [20][22] found that in rectus femoris different regions are more involved in different phase of the task of interest, in particular proximal region is more activated during hip flexion and distal region is more involved during knee extension.

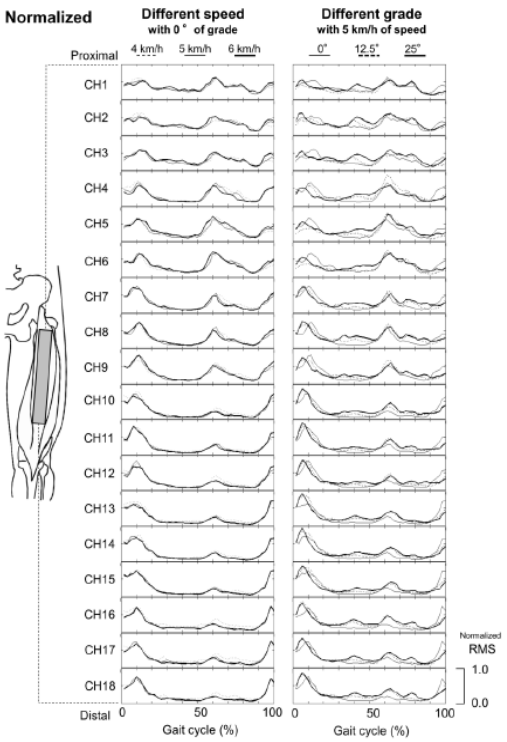

Figure 3.7: : picture from Watanade et al. [20] – analysis of RF activity during gait on a treadmill: distal region seems to be more involved at the beginning and at the end of gait cycle, while proximal portion is more active during hip flexion, just before the beginning of swing phase.

The localized activation within Rectus Femoris proximal and distal region during cycling was also discussed by Watanabe et al.[22]. Different workloads and pedal straps were adopted to analyse the activity of the muscle. They showed that the proximal region is more involved during the first half of the upstroke, when hip flexion occurs; the distal portion is more active during the downstroke, with knee extension (see Figure 3.8).

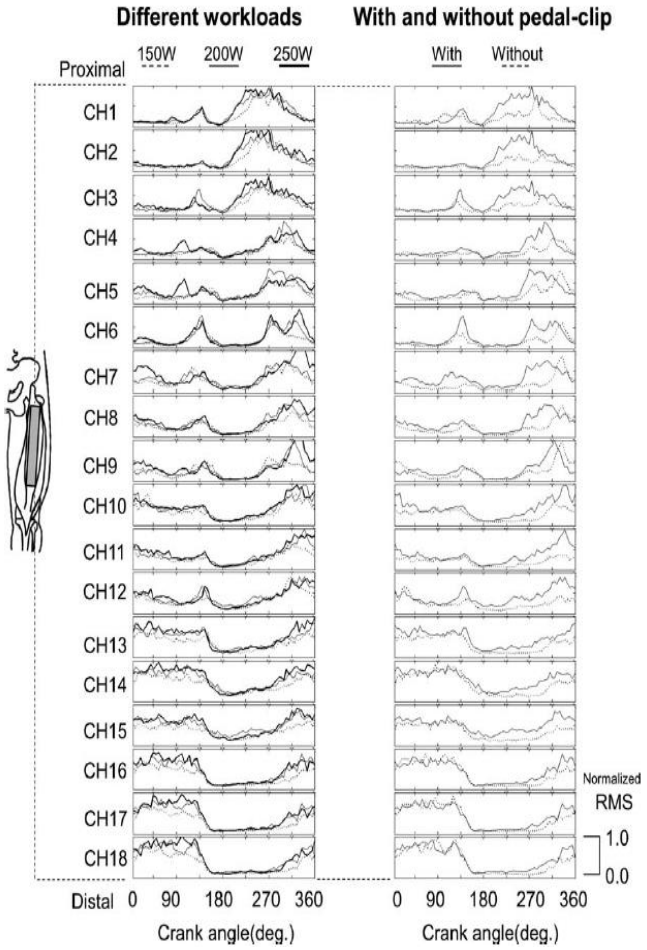

Figure 3.8: Watanabe et al. [22] analysis of Rectus Femoris regional-specific activation during cycling, proximal region is more involved during the first half of upstroke, when hip flexion occurs; distal portion is more active during downstroke, with knee extension.

- Gastrocnemius Medialis is a biarticular pennate muscle that is involved both in knee flexion and plantar flexion. Some studies (Hodson-Tole et. al [23], Watanabe et. al [24]) support the hypothesis that GM can be regionally recruited during a specific task, due to different orientations of the fibers within the mascle (Figure 3.9), in fact, fibers located in the distal region are closer to Achilles' tendon, this fibers are also less pennate than those in proximal region, so it has been suggested that distal region is more involved during ankle plantar flexion

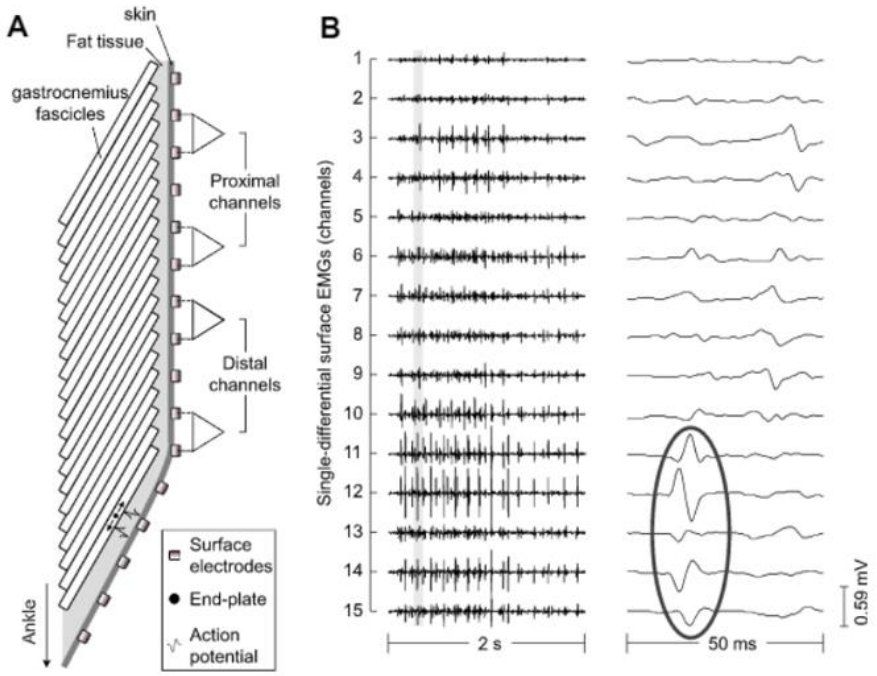

Figure 3.9: (picture from Hodson-Tole et al. [23] study): this is a representation of how different orientations of fibers within Gastrocnemius Medialis influence the patterns of the recorded signals at different proximal and distal regions. Signal propagation is highlighted in channels 11-15 (B).

- Vastus Medialis was investigated by Cabral et al. [26], the discharge rates of motor units belonging to proximal and distal region were identified and then cross-correlated. Authors found out that firing of MUs in the same VM region are much more cross-correlated than firing of MUs located in different regions. This suggests that proximal-distal VM regions could be modulated independently one from another in accordance with Gallina et al. [28] and Cabral et al. [27] (Figure 3.10).

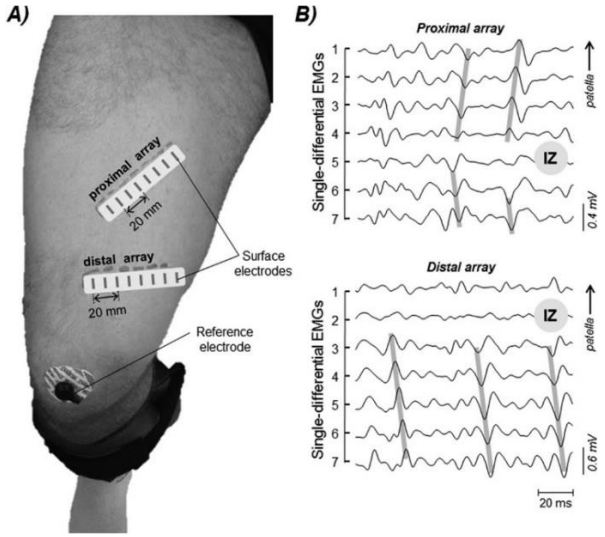

Figure 3.10: picture from Cabral et al. [25] that shows different discharge rate of fiber belonging to different regions. Innervation zone (IZ) is highlighted by shade circles and the propagation by thick grey lines

- Soleus was deeply investigated in Staudemann et al. [27], they showed that medial and lateral regions of this muscle are selectively activated during foot eversion and inversion. Soleus has a significant role with Gastrocnemius Medialis during late stance phase in gait as plantar flexor and at the end of upstroke and beginning of downstroke in cycling.

With this work we want to perform muscle synergies extraction with high-density EMG technique, in order to sample the signal from different bi-articular muscles regions and investigate the possible effect on electrode positioning on muscle synergy extraction. Rectus Femoris and Gastrocnemius Medialis is the focus of this analysis. As regards Soleus and Vastus Medialis, the different portions were treated as different muscles and EMG signals were detected from two couples of electrodes per muscle.

4 Materials and methods

4.1 Subjects

Eight healthy, male subjects were recruited to participate in this study (age: 26.4 ± 0.9 years, height: 177.6 ± 5.1 cm and body mass: 69.6 ± 4.6 kg). Before the beginning of any tests every subject has been properly instructed about the protocol and he was asked to sign an informed consent.

4.2 Experimental protocol

The protocol consisted of two tasks: over ground walking and cycling.

For walking task subject was asked to walk back and forth along a 10 m walkway for two minutes at natural pace. Mean walking velocity was equal to 3.4 ± 0.5 km/h for. After this trial they were asked to perform a cycling task on a vertical cycle ergometer (Reeharun 1400 Chinesport, Fig 4.1) at 60 rpm with fixed resistance (150 W) without pedal straps for one minute.

Figure 4.1: vertical cycle ergometer (Reeharun 1400 Chinesport)

Kinematics data were acquired through a Vicon optoelectronic system with 12 infrared cameras synchronixzed wirth EMG acquisition from lower limb muscles.

4.3 Kinematics: motion capture and marker positioning

For kinematic data collecting Vicon system was used. It consists of 12 infrared cameras (Vero 2.2), Vicon active wand for camera calibration, a PC with Nexus (software for kinematic data acquisition and elaboration). 16 reflective markers were placed on precise anatomical landmarks in accordance with Plug-in Gate lower body model. Joint angle and markers trajectories were calculated. A table with the positioning of the markers is reported below.

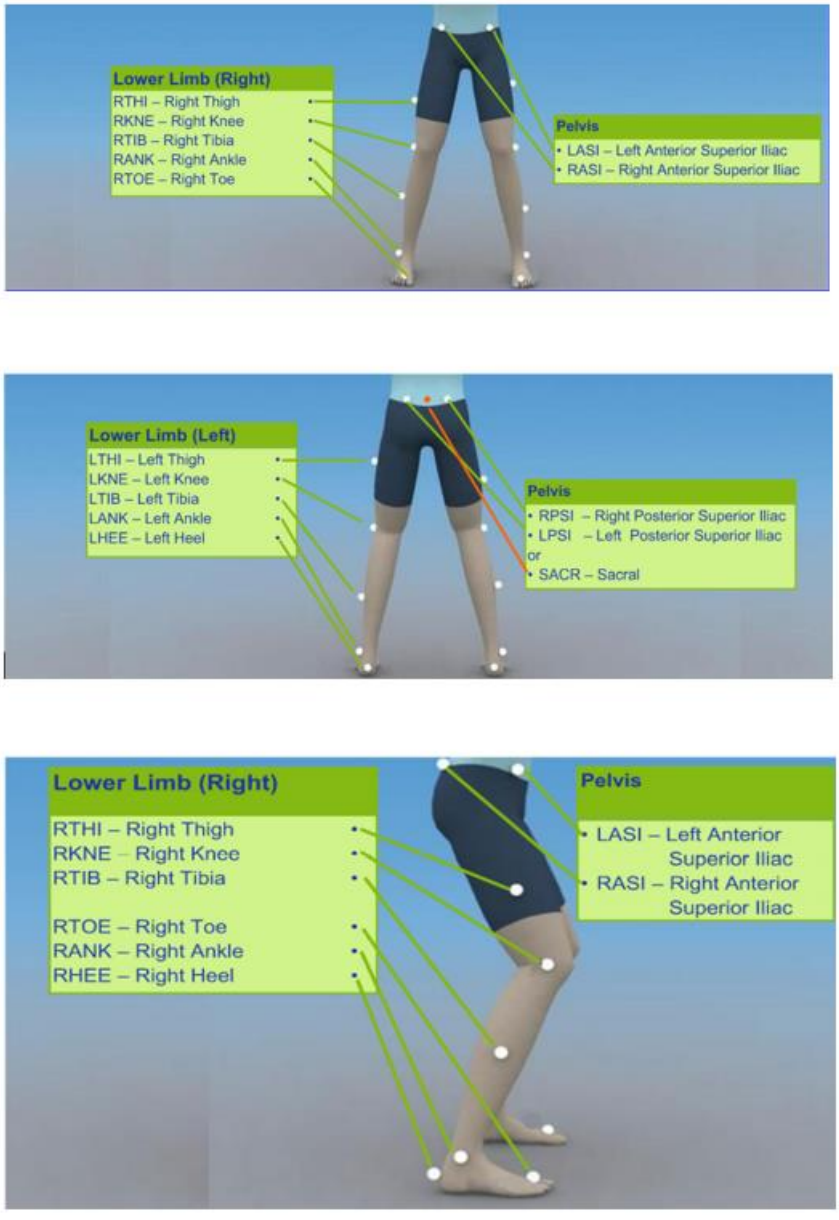

Figure 4.2: Indication for marker location (Vicon Nexus User Guide)

MARKER LABEL	DESCRIPTION	LOCATION ON SUBJECT
LTHI	Left thigh	Over the lower lateral 1/3 surface of the left thigh
LKNE	Left Knee	On the flexion-extension axis of the left knee
LTIB	Left tibia	Over the lower lateral 1/3 surface of the left shank
LANK	Left Ankle	On the lateral malleolus along an imaginary line that passes through the transmalleolar axis
LHEE	Left heel	On the calcaneus at the same height above the plantar surface of the foot as the toe marker
LTOE	Left toe	Over the second metatarsal head
RTHI	Right thigh	Over the upper lateral 1/3 surface of the left thigh
RKNE	Right Knee	On the flexion-extension axis of the left knee
RTIB	Right tibia	Over the upper lateral 1/3 surface of the left shank
RANK	Right Ankle	On the lateral malleolus along an imaginary line that passes through the transmalleolar axis
RHEE	Right heel	On the calcaneus at the same height above the plantar surface of the foot as the toe marker
RTOE	Right toe	Over the second metatarsal head
LASI	Left ASIS	Left anterior superior iliac spine
RASI	Right ASIS	Right anterior superior iliac spine
LPSI	Left PSIS	Left posterior superior iliac spine
RPSI	Right PSIS	Right posterior superior iliac spine

Table 4.1: Markers location on the subjects

4.4 Selected muscles

EMG signals were collected form lower limb muscles using bipolar or High-Density EMG.

Since the main goal of this thesis work was to investigate the effect of electrode positioning along RF and GM muscles on extracted synergies EMG from Rectus Femoris and from Gastrocnemius Medialis were acquired using HD-sEMG while for the other muscles a standard bipolar system was used. The studied muscles together with their main functional role are listed below.

- Rectus Femoris (RF): is a hip flexor and a knee extensor, is more involved at midstance and initial swing phases during gait, final upstroke, and initial downstroke during bike.
- Gastrocnemius Medialis (GM): is a plantar flexor and it contributes to knee flexion. It is mainly involved during late stance of gait cycle and downstroke phase during cycling.

- Vastus Medialis (VM): is a knee extensor that is activated during gait at midstance phase and initial downstroke phase of pedalling cycle.
- Soleus (SOL): has a significant role with Gastrocnemius Medialis during late stance phase as a plantar flexor and initial downstroke during pedalling.
- Gluteus Medius (GMed): is a hip flexor and abductor, it is mainly activated during stance phase in gait and during upstroke and downstroke during cycling.
- Biceps Femoris (BF): is a hip extensor and knee flexor, its activity is evident during terminal swing and initial stance phase in gait cycle and during downstroke in cycling.
- Vastus Lateralis (VL): is a knee extensor that is engaged in gait during initial swing phase and in cycling during initial downstroke phase.
- Tibialis Anterior (TA): is an ankle dorsiflexor and it is more involved during early stance phase in gait and final upstroke phase in cycling.

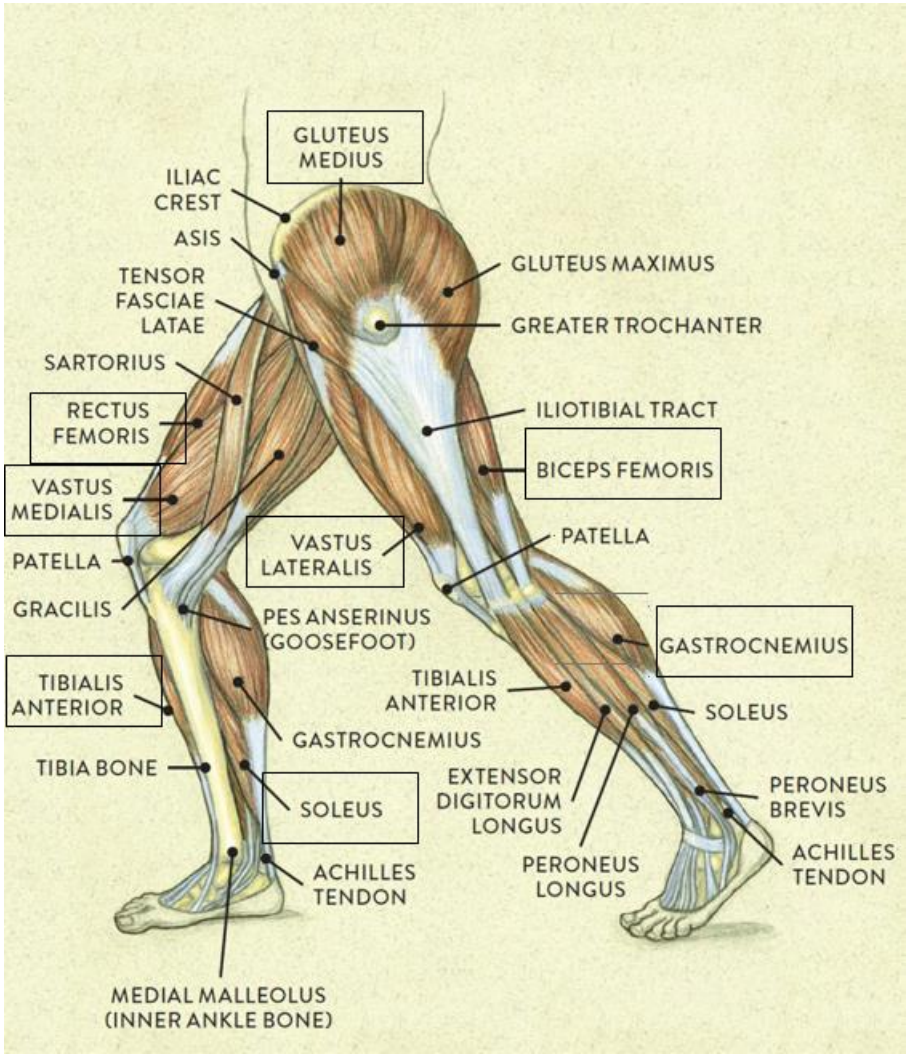

Figure 4.3: selected muscles for experimental protocol

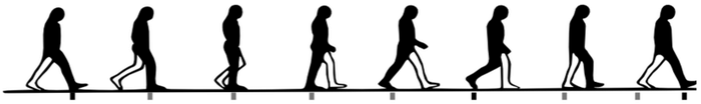

	Stance phase					Swing phase		
	Double support	Simple support			Double support			
		Initial	Middle	Terminal		Initial	Middle	Ter.
ILIACUS								
SARTORIUS								
GRACILIS								
RECTUS FEMORIS								
ADDUCTOR LONGUS								
VASTI								
GLUTEUS MAXIMUS								
GLUTEUS MEDIUS								
BICEPS FEMORIS								
TIBIALIS ANTERIOR								
EXTENSOR DIGITROUM LONGUS								
GASTROCNEMIUS								
SOLEUS								
FLEXOR HALLUCIS LONGUS								
TIBIALIS POSTERIOR								
PERONEUS LONGUS								

Figure 4.4: Activation intervals of lower limb muscles during gait.

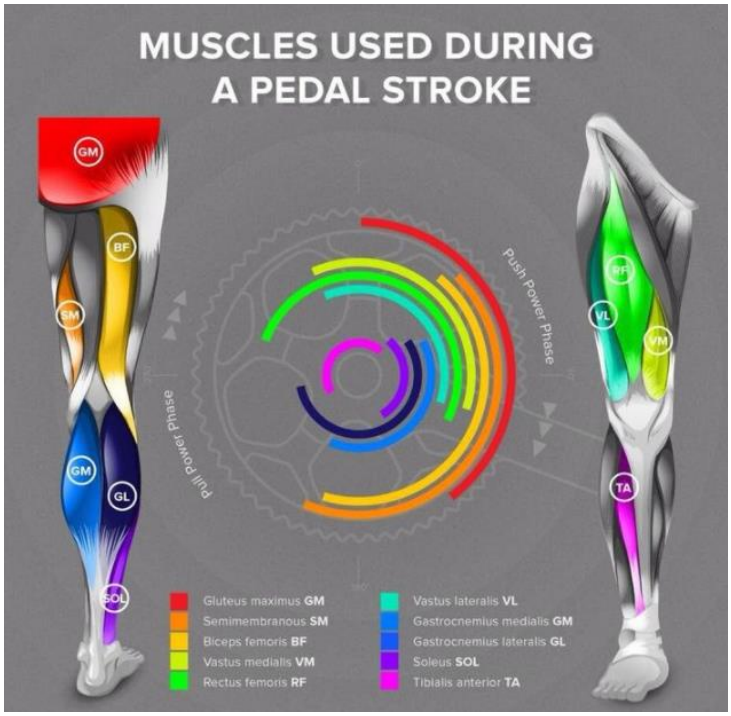

Figure 4.5: Activation intervals of lower limb muscles during cycling.

4.5 Skin preparation and electrode positioning

Flexible Kapton 16x2-electrode matrices with IED 1.5 cm were adopted on RF and GM, while disposable bipolar electrodes were placed on the other muscles. A double-adhesive foam was necessary to create an adhesive surface with the skin; a thin layer of conductive paste was spread on the foam, after it was positioned on the matrix. No foam was necessary for bipolar electrodes. Before placing matrix and electrodes the hair was removed and subject's skin was scrubbed with an abrasive paste.

A precise electrode positioning for each muscle is required in accordance with the fibers' architecture and orientation:

- Rectus Femoris: electrode matrix was placed in accordance with the positioning defined by Watanabe et al. [21]. The distal end of the muscle was identified by palpation, the correct matrix orientation is along the line between the anterior superior iliac spine and the superior edge of patella (Fig. 4.6). SENIAM recommendation: at 50% of the line from anterior iliac spine to the superior part of the patella.

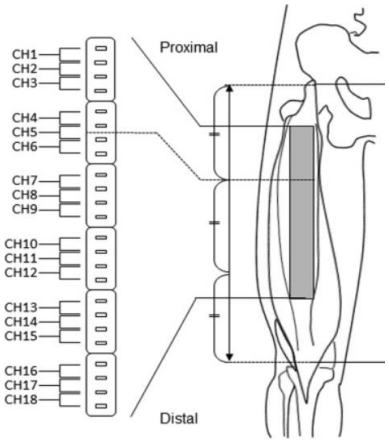

Figure 4.6: (picture from Watanabe et al. [23]): indication of electrodes matrix positioning on the rectus femoris

- Gastrocnemius Medialis: F.V. Dos Anjos et al. [28] showed a precise indication of an electrodes array positioning, the most proximal electrode was located 2 cm distally to the popliteal fossa, aligned parallel to the longitudinal axis of the muscle (Fig. 4.7). SENIAM standard positioning: on the most prominent bulge of the muscle.

- Soleus: F.V Dos Anjos et al. [28] showed indications for an effective electrode positioning on this muscle, these are valid for both medial and lateral regions. First, the distal end of the medial gastrocnemius was identified, the first electrode was positioned a few millimetres below this point, the other was positioned at 45° towards the inside of the lower part of the muscle, 3 cm below the first electrode. IED 2 cm (Fig. 4.7).

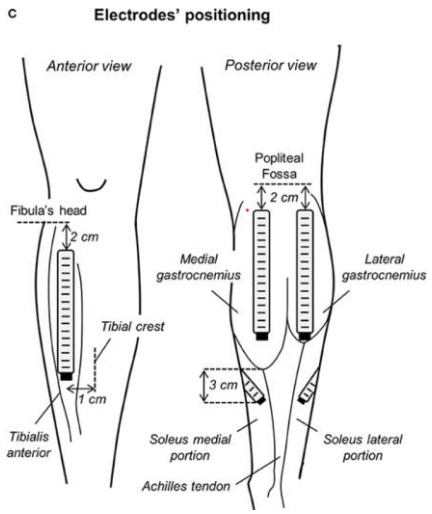

Figure 4.7: (picture from F.V Dos Anjos et al. [28]): a simple representation of electrodes positioning on Gastrocnemius Medialis and Soleus.

- Vastus Medialis: A couple of bipolar electrodes was placed on its proximal portion, where the fibers form a slight angle with the longitudinal axis of the thigh; because of the fibers close to the patella increase their pennation angle, a second couple of bipolar electrodes was placed transversely with respect the first one. (H.V. Cabral et al. [25]) (Fig. 4.8).

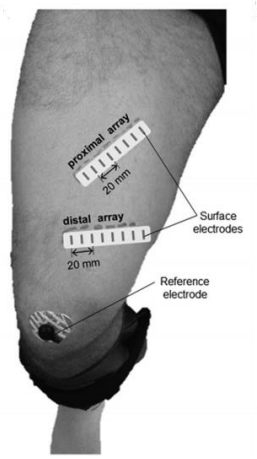

Figure 4.8: (picture from Cabral et al. [25]): indication for electrodes location on Vastus Medialis, in this study two couple of bipolar electrodes has been used, instead of electrodes array.

- Gluteus Medius: SENIAM positioning was adopted, electrodes need to be placed at 50% on the line from the crista iliac and the trochanter. Recommended IED is 2 cm (Fig. 4.9).

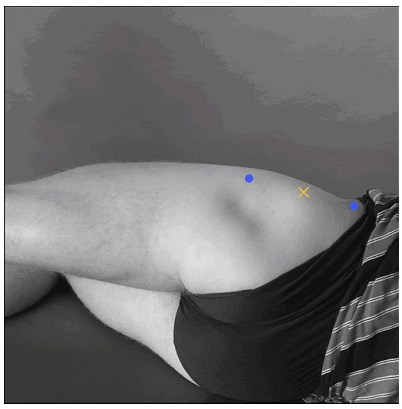

Figure 4.9: SENIAM indication for electrodes location on Gluteus Medius.

- Biceps Femoris: SENIAM positioning was chosen. The electrodes need to be placed at 50% on the line between the ischial tuberosity and the lateral epicondyle of the tibia, in direction of this line. IED 2 cm (Fig. 4.10).

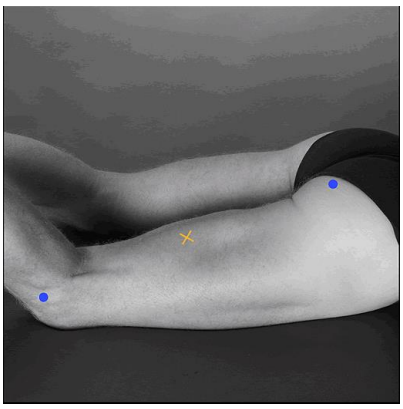

Figure 4.10: SENIAM indication for electrodes location on Biceps Femoris.

- Vastus Lateralis: SENIAM positioning was adopted. Electrodes need to be placed at 2/3 on the line from the anterior superior spina iliac to the lateral side of the patella, in the direction of muscle fibers. Recommended IED 2 cm (Fig. 4.11).

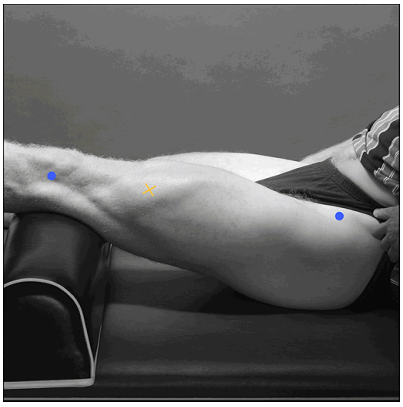

Figure 4.11: SENIAM indication for electrodes location on Vastus Lateralis.

- Tibialis Anterior: SENIAM positioning was chosen. The electrodes need to be placed at 1/3 on the line between the tip of the fibula and the tip of the medial malleolus. IED 2 cm (Fig. 4.12).

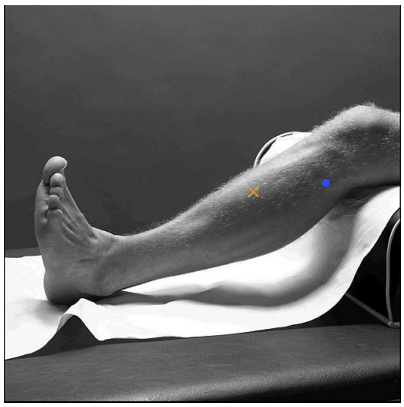

Figure 4.12: SENIAM indication for electrodes location on Tibialis Anterior.

- Reference electrode was necessary for MEACs probes only and must be placed on a bony prominence, patella in this case.

4.6 EMG detection system

For EMG signals acquisition two different systems were used: MEACs probes for HD-sEMG from RF and GM, DuePro for single differentials from the other muscles.

DuePro is an instrument consisting in seven wireless probes (Due) a charging station (Due Station) and a wireless probe for the acquisition of digital or analog signals (DueBio). Due probes are designed to pick up two sEMG through two pairs of bipolar electrodes, DueBio is a probe for the collection of biomechanical and kinematic signals, in this work it was used to acquire a common trigger signal. Signals from DuePro system were visualised with a MATLAB interface.

The detection system used to acquire High Density EMG is called MEACs (Multichannel EMG Acquisition System) produced by LiSiN (Laboratorio di Ingegneria del Sistema Muscolare), Turin. It is a wearable system that allows to acquire sEMG signals in monopolar configuration[21]. The system has 32 channels for EMG acquisition and the 33rd allows to acquire an external trigger. It's able to communicate via Wi-Fi with a PC for online signal visualisation using bp® software.

Trigger was necessary to synchronize EMG from MEACs and DuePro, and kinematic data from motion capture. The trigger was generated by the Vicon system with a level transition when acquisition started and anew transition when acquisition ended. EMG acquisition started first, so the trigger could be visualized on bp and MATLAB interface, in this way it was possible to synchronize EMG signals and kinematic data.

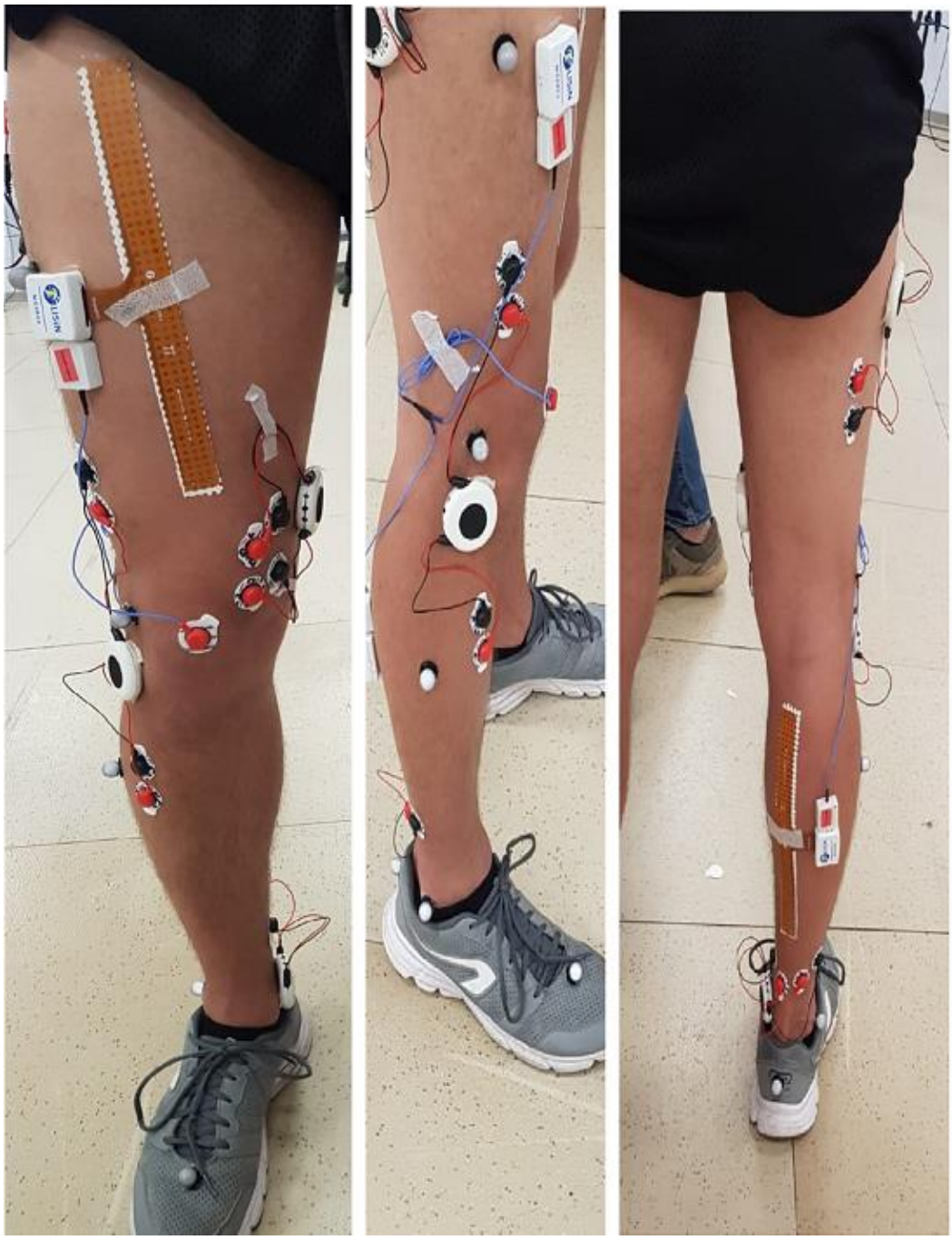

Figure 4.13: Complete set-up applied on a subject. Two electrode matrices are placed on Rectus Femoris and Gastrocnemius Medialis, bipolar electrodes are placed on Biceps Femoris, Gluteus Medius, Tibialis Anterior, Vastus Lateralis, Vastus Medialis (one couple on the proximal region and one on the distal region) and Soleus (one couple on the medial region and one on the lateral region), 16 reflective markers are placed in accordance with Plug-in Gate lower body model

4.7 EMG processing and muscle synergies extraction

EMG and kinematics data processing:

- EMG signals were sampled at 2048 Hz, the first and last part of the signals in correspondence of trigger edges were removed (Figure 4.15).

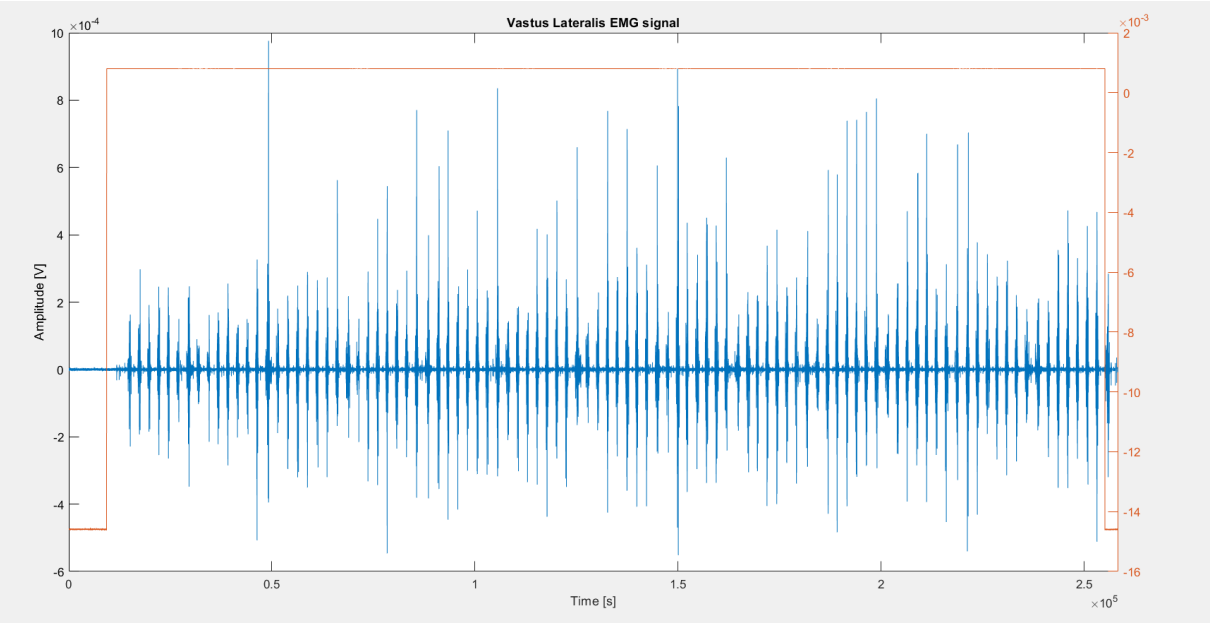

Figure 4.14: Signal from Vastus Lateralis during walking before removing the portions in correspondence of the trigger edges.

- Single differential signals from RF and GM were calculated along the muscle (Longitudinal Single Differential see Figure 4.17). To simulate electrode dimensions, usually used for gait analysis, electrodes with a dimension of 1.5x1.5 cm were simulated by calculating the mean of the monopolar signals recorded by four neighbour electrodes (refer to Figure 4.16 for more details). One pair of simulated electrodes in proximal position, one in distal position and one couple in the middle (simulating the SENIAM standard positioning) were used to calculate the longitudinal single differentials with IED 1.5 cm, that fits very well to investigate a selective detection volume. Proximal, medial, and distal positions were defined as the ones at the 20%, 45% and 70% of the thigh length for RF and the shank length for GM.

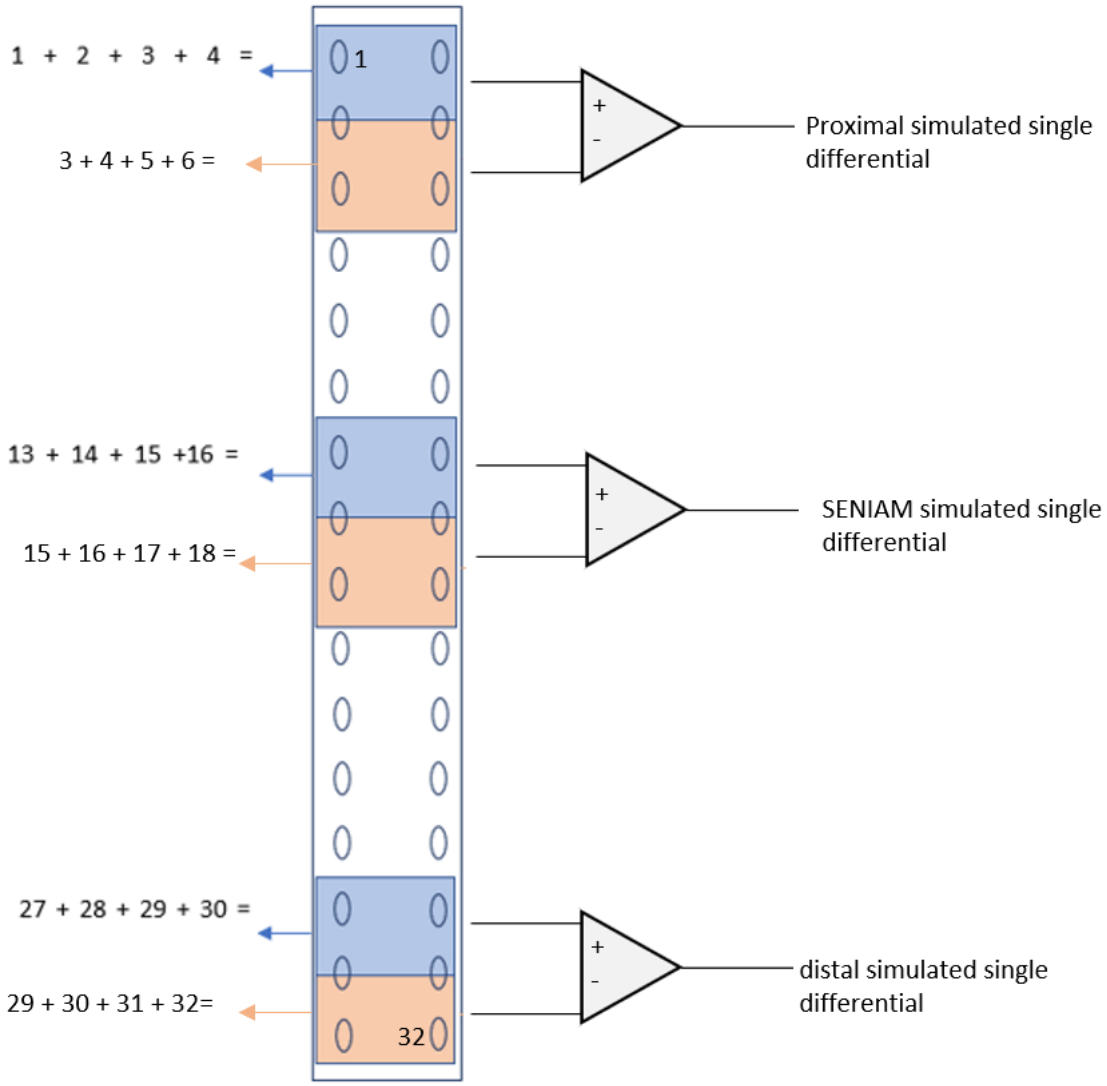

Figure 4.15: : Graphical description of how RF and GM signals were elaborated. Four signels recorded from neighbour electrodes were summed together simulating the detection of monopolar signal using electrodes with dimension 1.5x1.5 cm; then single differentials are calculated from difference of all possible monopolar couple with IED 1.5 cm. 14 single differentials were obtained; one proximal, one medial and one distal single differential were selected .

Figure 4.16: Single differentials from GM (top) and RF (down) calculated from monopolars with electrode dimension 1.5x1.5 cm and IED 1.cm.

- Signals were bandpass filtered between 20 Hz and 350 Hz, that is the frequency range where most of power density of EMG is found, 20 Hz were chosen as low cut-off frequency to reduce the motion artefacts. Signals acquired during cycling were corrupted by power line noise, so they were filtered using a notch filter to remove 50 Hz and multiples. Signals were rectified and lowpass filtered using a Butterworth 4nd order filter with a cut-off frequency 10 Hz (Olivera et al. [30]) to calculate EMG envelopes (Figure 4.17).

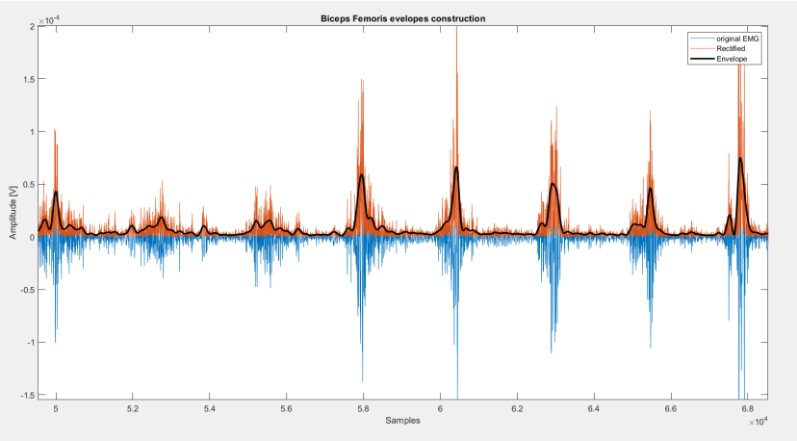

Figure 4.17: an example of EMG envelope construction; in this figure original signal (blue), rectified (red) and envelope (black) are overlapped.

- Knee flexion-extension, hip flexion-extension and ankle plantar/dorsiflexion angles were collected. The right heel marker trajectory was used to identify the task cycles and then segment the EMG envelopes and the joint angles. For gait, the minima were used to identify the heel strike events, that is the beginning of the gait cycle (Figure 4.19 top). For cyclig the minima identified the Bottom Dead Center that was considered as the beginning of the cycle (Figure 4.19 down).

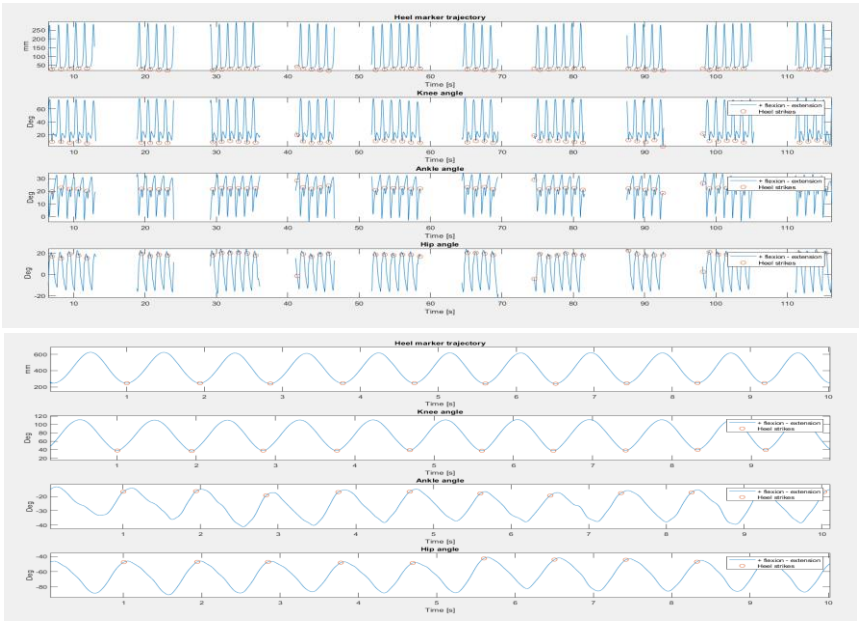

Figure 4.18: joint angle and heel marker trajectory during gait (top) and cycling (down). HEEL strike instant, Bottom Dead Center (red circles) and join angles are overlapped to highlight different cycles of the task.

- Every walking/cycling cycle was normalized in time downsampling the original signal length to 200 samples. For gait, U-turns were removed and the first cycle before and after each turn was removed to have only complete cycle.
- Finally, 10 cycles for each task were selected. Muscle synergies were extracted from averaging the ten cycles identified previously in accordance with Olivera et al. [30]. Each averaging envelope was normalized for its max value to not bias NNMF results.

- Mascle synergy extraction was performed maintaining SENIAM standard positioning on one muscle and changing the electrode positioning from proximal to distal on the other one. To identify the correct number of synergies a total VAF value of 0.90 (Kim et. al. [14], Wojtara et. al. [15] and Barroso et. Al. [17]). and VAF for individual muscle of 0.7 were chosen [16][17]. The extraction was repeated first using the total VAF only, then adding the VAF for individual muscle. The same number of synergies were extracted in both cases.

NNMF was applied using the dunction nnmf provided by MATLAB. NNMF algorithm parameters:

- Max number of iterations: 1000
- Termination tolerance on change in size of the residual: 10e-6
- Termination tolerance on change in the elements: 10e-6

A certain number of replicates for each iteration was necessary, because the algorithm could stick in local minimum, so muscle synergies extraction was repeated 40 times (Barroso et al. [17]) and the final value of H and W are the one that minimize the root-mean square residual calculated as below:

$$D = \frac{A - W * H}{||A - W * H||} * \frac{1}{\sqrt{N * M}}$$

Where A is the original EMG matrix, W and H are muscle synergies weights and activation coefficient, N and M are matrix A dimensions.

4.8 Chosen parameters for muscle synergies grouping

Two indicators have been used to group activation coefficient and weights extracted from different subject and conditions: Zero-Lag Cross Correlation and Cosine Similarity.

- Zero-Lag Cross Correlation ranges between -1 and 1 and is used to compare to activation coefficients. It is formulated as follows:

$$CC = \frac{R_{xy}[0]}{\sqrt{R_{xx}[0] * R_{yy}[0]}} \qquad Rxy = \int_{-\infty}^{+\infty} x(t) * y(t+\tau)dt$$

Where R_{xx} is the autocorrelation for the first activation coefficient, R_{yy} is the autocorrelation for the second activation coefficient and R_{xy} is the cross-correlation function. This parameter is calculated in MATLAB using xcorr function with *'coeff'* option.

- Cosine Similarity, ranges between 0 and 1 needs to verify the similarity between weight values, it confronts two different weight vectors calculating the normalized scalar product.

$$CS = \frac{W_i * W_j}{||W_i|| * ||W_j||}$$

Since the initial values of H and W are random these parameters are essential to overlap similar synergies from different subject to confront the results and check intra-variability among synergies from the same subjects using different electrodes positioning.
First, Zero-Lag Cross Correlation is calculated to find matching activation coefficient in muscle synergies of different subjects, if there is a correspondence similar muscle synergies could be compared in terms of weight values using Cosine Similarity.

5 Results

5.1 Muscle synergy extraction results - Gait

Muscle synergies were extracted from 5 subjects out of 8. Three subjects were excluded because of the presence of artefacts and noise affecting all signals.

5.1.1 Muscle synergy extraction changing electrode positioning along Rectus Femoris

In this section the results about differences in EMG detected from the proximal, SENIAM, and distal electrode positioning on the Rectus Femoris muscle are reported. The EMG signals for all other muscles (included Gastrocnemius medialis) are from the SENIAM positioning. Envelopes calculated from different electrode locations along Rectus Femoris showed that only 1 subject out of 5 have a localized activation of proximal portion of the muscle during hip flexion (approximately 60-70% of gait cycle) and distal region during knee extension in midstance phase. All remaining 5 subjects have shown little or no differences between proximal and distal Rectus Femoris' regions.

The results of two subjects showing different behaviours are reported in the following. Figures 5.1. and 5.2 shows the envelopes normalized in time and amplitude of ten gait cycles. For Subject 1 (fig. 5.1) EMG detected from the electrodes on the proximal RF region shows a clear activation during the hip flexion (highlighted with red circle); this activation can be appreciated also under the electrodes in SENIAM position, while it is absent for distal electrode positioning. Subject 4 (Fig. 5.2) does not show any difference between different electrode placements.

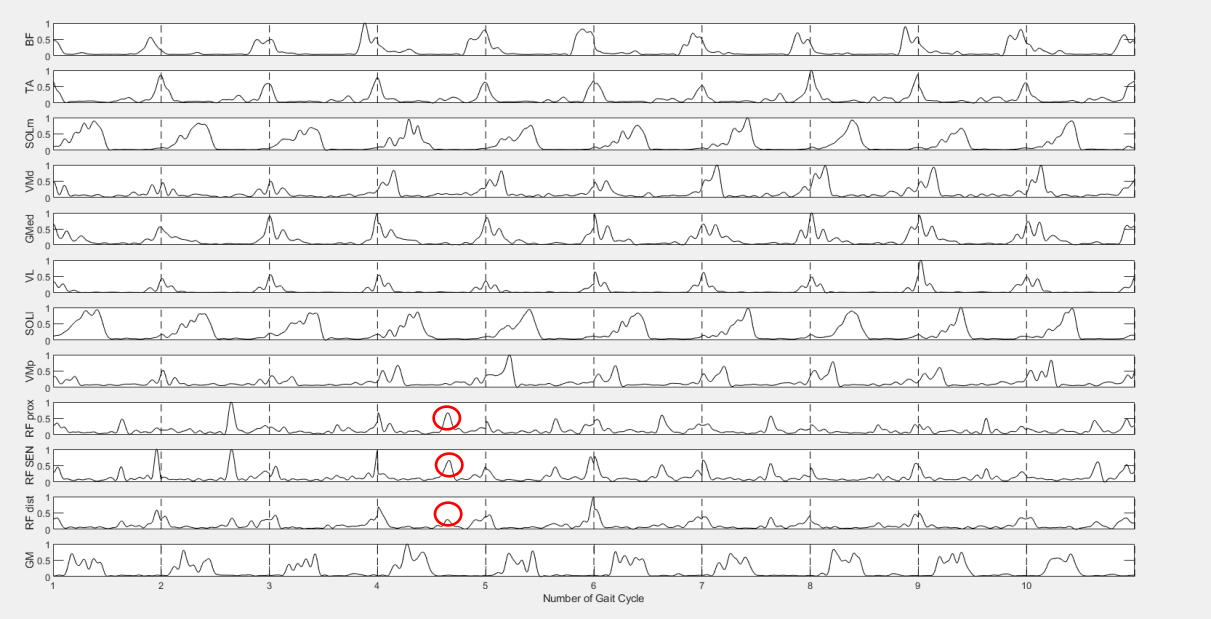

Figure 5.1: EMG envelopes for all muscles during ten gait cycles for Subject 1. The length of each gait cycle is normalized to 200 samples. The envelope for each muscle is normalized in amplitude with respect to the maximum of the envelope. On the x-axis the number of each gait cycle is reported. Red circles indicates the activation of RF during hip flexion, this activation can be appreciated when electrodes are placed in proximal and SENIAM position, it is absent for distal position.

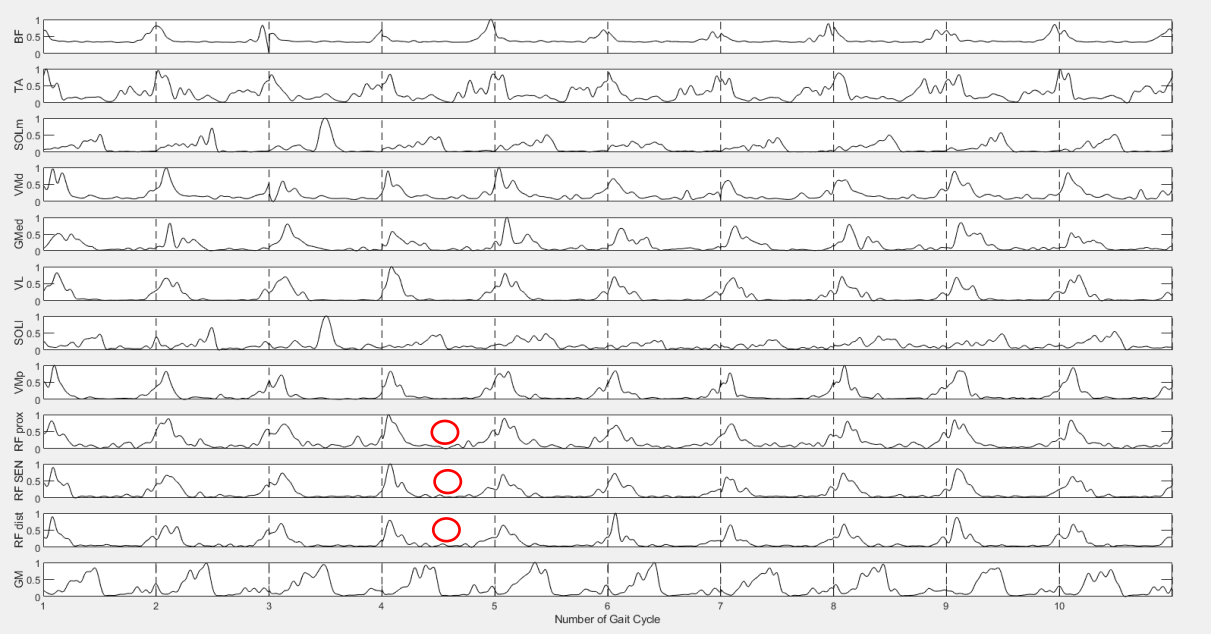

Figure 5.2: EMG envelopes for all muscles during ten gait cycles for Subject 4. The length of each gait cycle is normalized to 200 samples. The envelope for each muscle is normalized in amplitude with respect to the maximum of the envelope. On the x-axis the number of each gait cycle is reported. The acrivation of RF during hip flexion is totally absent as highlighted by re circles.

Figures 5.3 and 5.4 show the average envelopes for Subject 1 and 4.

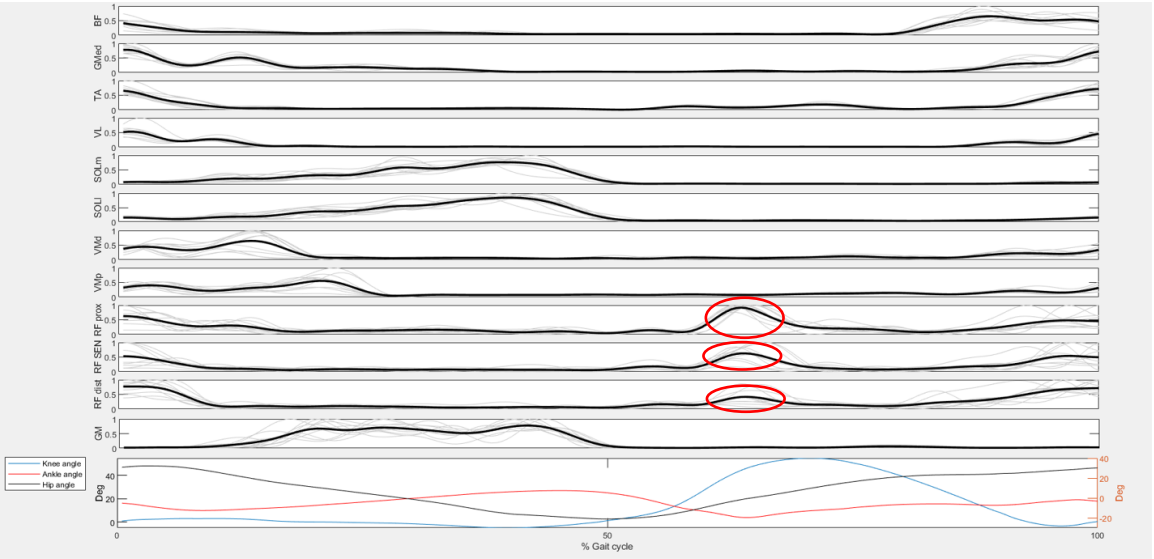

Figure 5.3: All cycle for each muscle of Subject 1 is overlapped and the mean calculated (thick black line). the mean behaviour of knee (blue), ankle (red) and hip (black) angles are reported. The activation of Rectus femoris during hip flexion is highlighted (red circle), this activation clearly decreases from proximal to distal position.

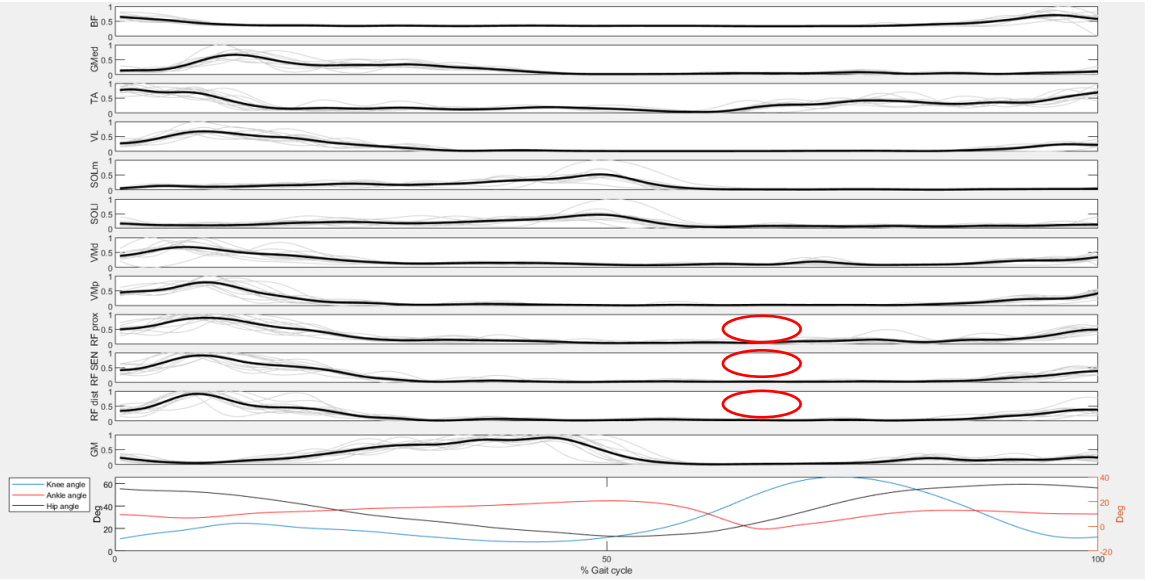

Figure 5.4: All cycle for each muscle of Subject 4 is overlapped and the mean calculated (thick black line). the mean behaviour of knee (blue), ankle (red) and hip (black) angles are reported. The activation of Rectus femoris during hip flexion is totally absent as highlighted (red circle).

In figures 5.5 and 5.6 RF mean envelopes, muscle synergy activation coefficients and weights and RF reconstructed envelopes for Subject 1 and 4 are shown.

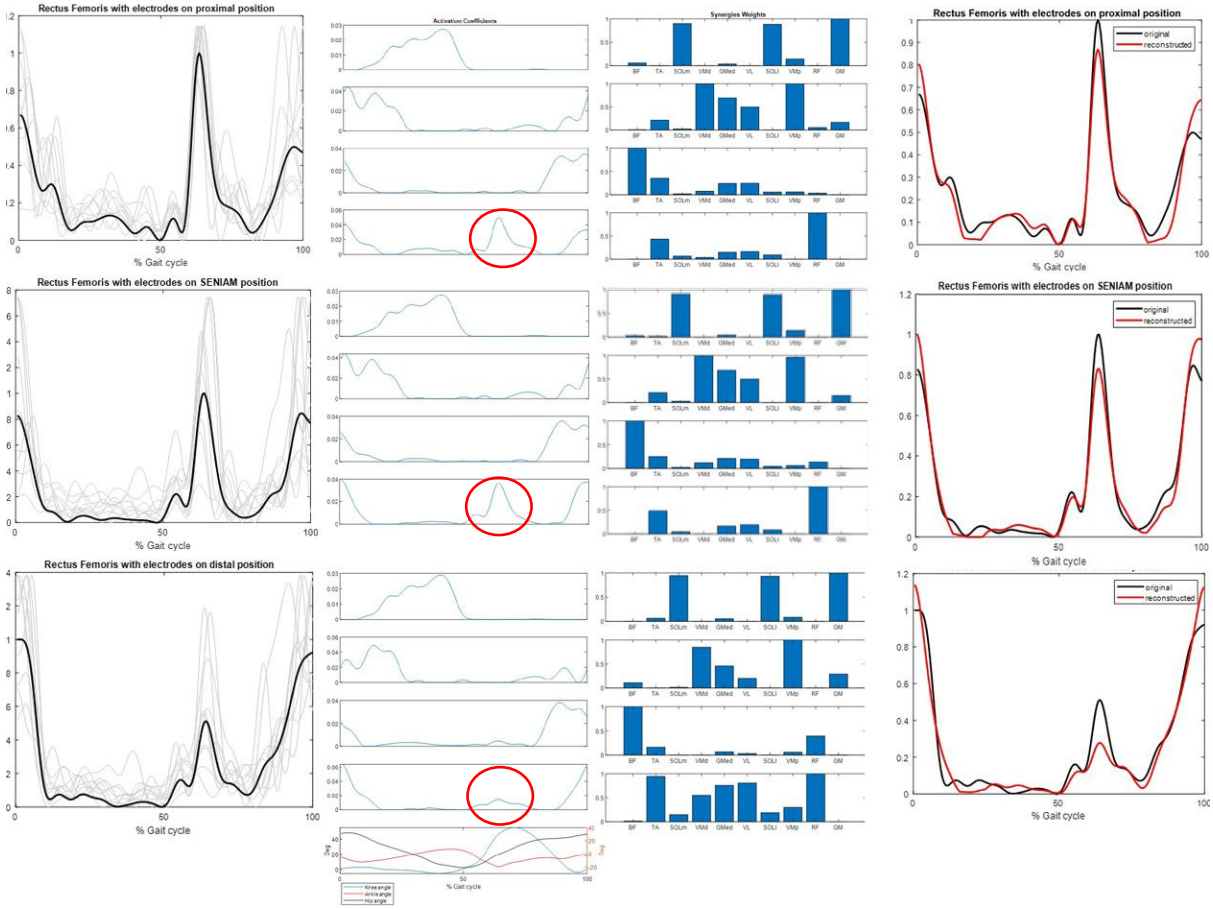

Figure 5.5: muscle synergy extraction results for Subject 1. Left column shows all RF overlapped envelopes and the average one (thick black line). central column shows the four extracted muscle synergies for the three different electrode positioning and joint angle graph. Right column shows average envelope and the reconstructed one, VAF of 0.90 provides a good quality of reconstruction. Rectus femoris contribution is mainly present in Synergy 4. The coefficients of Synergy 4 show a peak between 60% and 80% of the gait cycle (when hip flexion occurs) whose amplitude decreases moving from proximal to distal position.

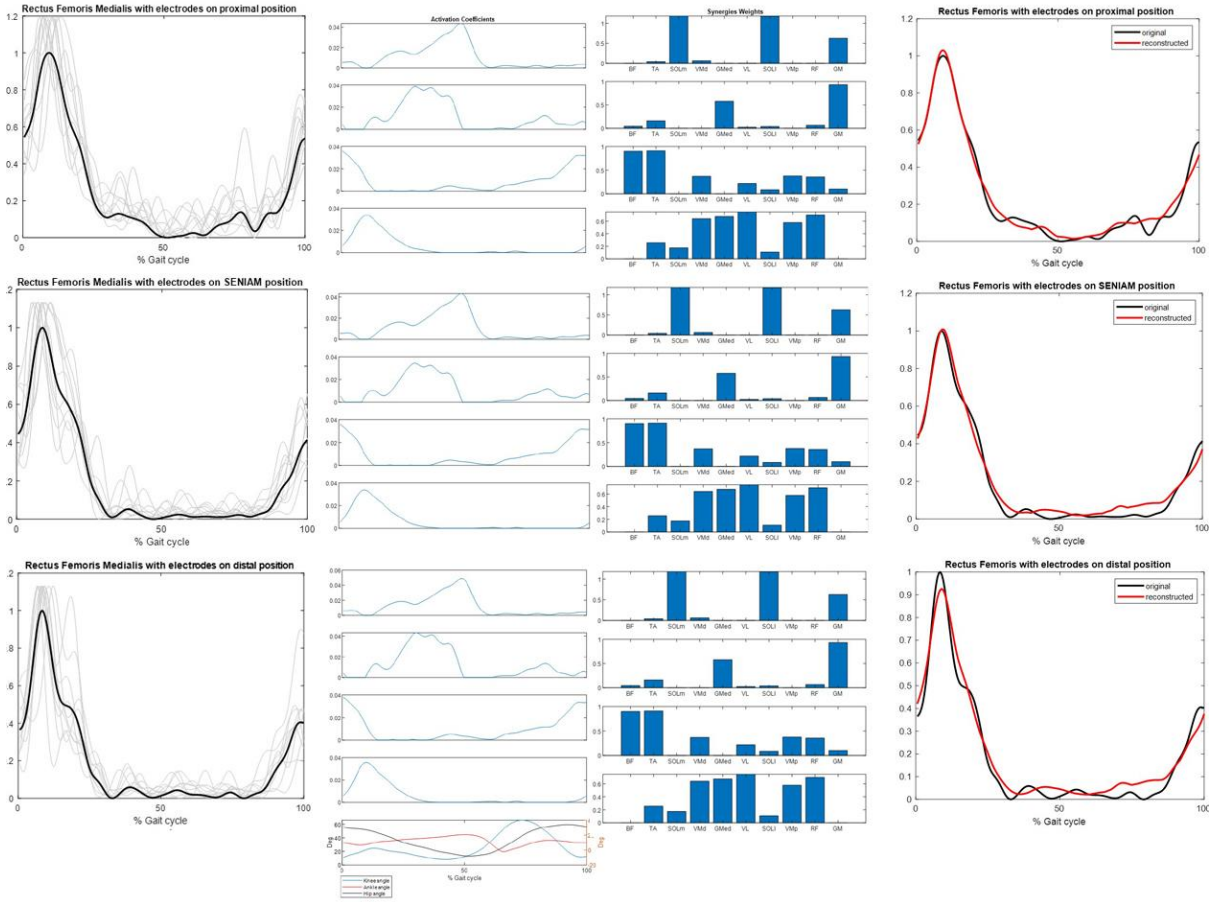

Figure 5.6: muscle synergy extraction results for Subject 4. Left column shows all RF overlapped envelopes and the average one (thick black line). central column shows the four extracted muscle synergies for the three different electrode positioning and joint angle graph. Right column shows average envelope and the reconstructed one, VAF of 0.90 provides a good quality of reconstruction. Synergy 4, that represent RF activity, activation coefficient and weights are the same for the three positions.

Comparing these results with previous studies in literature [17][13], the extracted muscle synergies during gait show common behaviours: as described in Chapter 3.5, Synergy 1 from figure 5.5 represents Gastrocnemius Medialis activity and Soleus during late stance and pre-swing phases. Synergy 2 mainly represents stance phase, where Gluteus Medius, Vastus Medialis and Vastus Lateralis are mainly involved. Synergy 3 is characterized by the activation of Biceps Femoris during late swing phase. Synergy 4 describes the activity of Rectus Femoris Tibialis Anterior, Vastus Medialis and Lateralis at midstance and initial swing phases.

Rectus Femoris is mainly represented by the fourth synergy for both subjects. As we can see from figure 5.5 (referred to Subject 1) moving the electrodes from proximal to distal region both weights and activation coefficients change. When the electrodes are placed over proximal portion of the muscle there is a peak of activity at 60-70% of gait cycle, corresponding to hip flexion. These peak decreases if a distal electrode positioning is adopted. Subject 4 (fig. 5.6) does not show different activation pattern changing the electrode positioning and the activity of RF during hip flexion cannot be appreciated.

Cosine similarity is calculated to quantify the variation of synergy weights.

Synergies	Subject	CS prox-SENIAM	CS prox-dist	CS dist-SENIAM
Synergy 1	**1**	**0.9998**	**0.9977**	**0.9986**
	4	**1**	**0.9989**	**0.9987**
Synergy 2	**1**	**0.9992**	**0.9619**	**0.9578**
	4	**0.9992**	**0.9619**	**0.9578**
Synergy 3	**1**	**0.9898**	**0.8999**	**0.9403**
	4	**0.9984**	**0.9985**	**0.9991**
Synergy 4	**1**	**0.9979**	**0.8061**	**0.8166**
	4	**0.9972**	**0.9957**	**0.9992**

Table 5.1: cosine similarity calculated from synergy weights obtained changing electrode positioning along RF. as highlighted in yellow synergy 4 of Subject 1 is the only one with value of CS not above 0.90. Subject 4 does not show CS lower than 0.90.

As highlighted in yellow (Table 5.1) Subject 1 shows Cosine similarity values below 0.90 (common threshold shown in literature [33]) for the Synergy 4. Comparing the weights for the fourth synergy between proximal and SENIAM electrode positioning the value of CS is very high, in fact the proximal activation pattern is still present moving the electrodes over the central portion of the muscle, while this value decreases between proximal and distal, and between SENIAM and distal electrode location, where the activation during hip flection is lower. On the other hand, subject 4 doesn't show any difference in synergy weights, as evidenced by Cosine similarity values.

5.1.2 Muscle synergy extraction changing electrode positioning along Gastrocnemius medialis

In this section the results about differences in EMG detected from the proximal, SENIAM, and distal electrode positioning on the Gastrocnemius Medialis muscle are reported. The EMG signals for all other muscles (included Rectus Femoris) are from the SENIAM positioning. No subject showed a different activation of Gastrocnemius Medialis moving from proximal to distal region, for this reason muscle synergies from only one representative subject are reported. Figures 5.7 the envelopes normalized in time and amplitude of ten gait cycles for Subject 1.

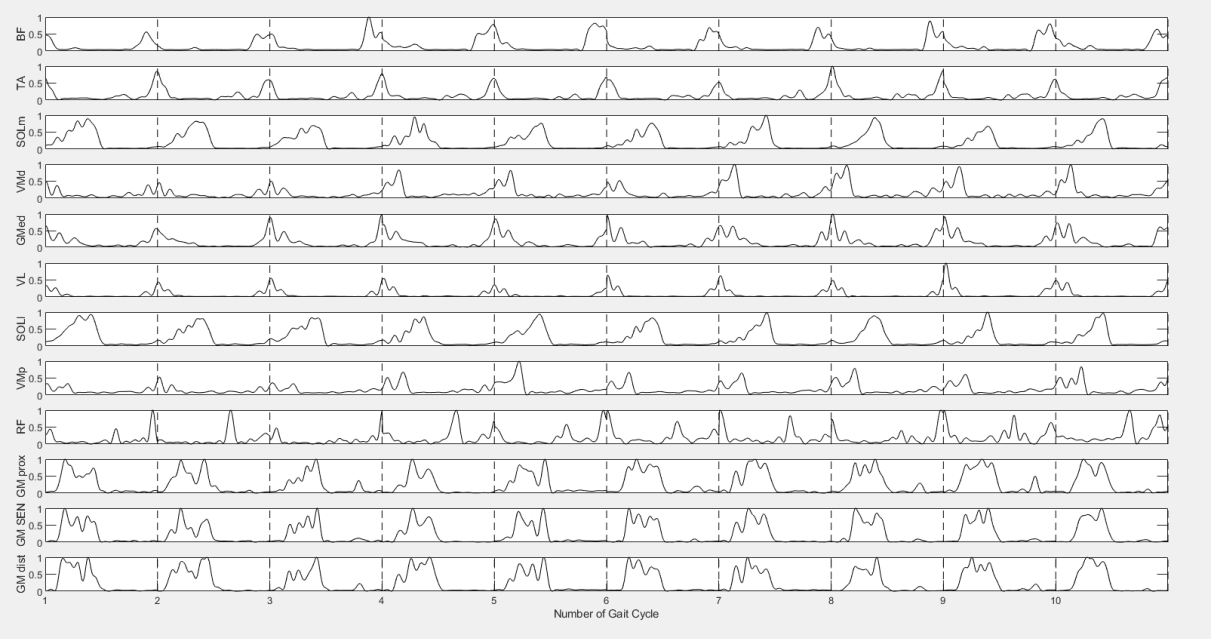

Figure 5.7: EMG envelopes for all muscles during ten gait cycles for Subject 1. The length of each gait cycle is normalized to 200 samples. The envelope for each muscle is normalized in amplitude with respect to the maximum of the envelope. On the x-axis the number of each gait cycle is reported. There is not evident difference in GM activation pattern.

Muscle synergy extraction was performed using the mean envelope estimated on ten gait cycles. Figure 5.8 shows the average envelopes for Subject 1.

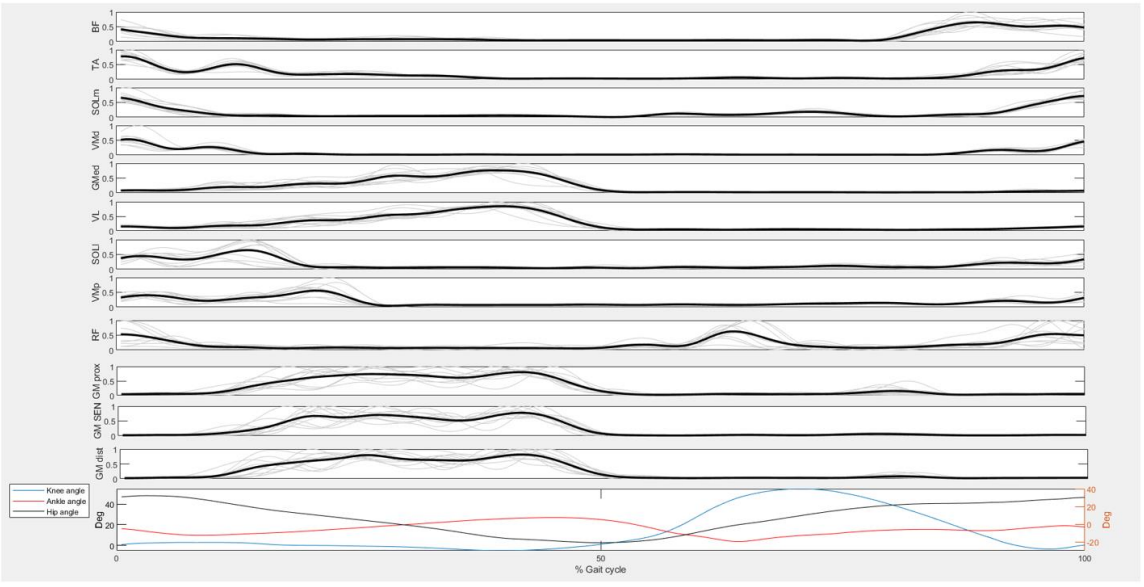

Figure 5.8: All cycle for each muscle of Subject 1 is overlapped and the mean calculated (thick black line). the mean behaviour of knee (blue), ankle (red) and hip (black) angles are reported. GM activation from different electrode positioning seems to be very similar.

In figures 5.9 GM mean envelopes, muscle synergy activation coefficients and weights and RF reconstructed envelopes for Subject 1 and 4 are shown.

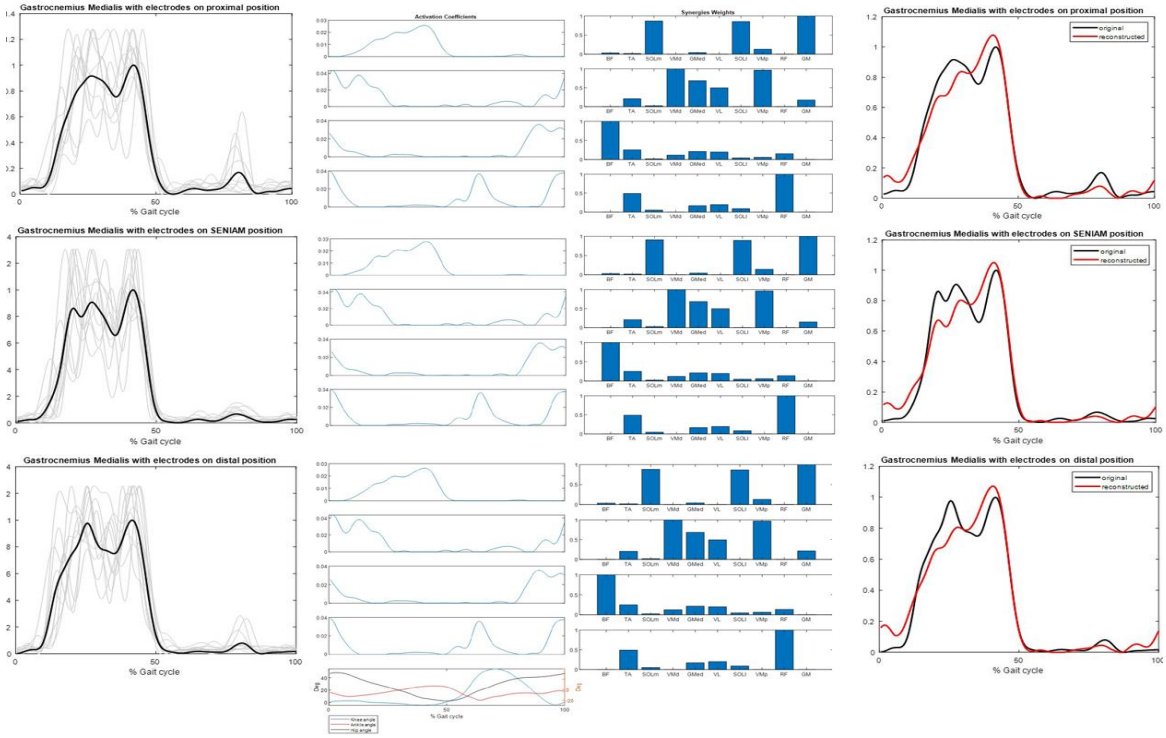

Figure 5.9: muscle synergy extraction results for Subject 1. Left column shows all GM overlapped envelopes and the average one (thick black line). central column shows the four extracted muscle synergies for the three different electrode positioning and joint angle graph. Right column shows average envelope and the reconstructed one, VAF of 0.90 provides a good quality of reconstruction. Synergy 1, that represent GM activity, activation coefficient and weights are the same for the three positions.

Gastrocnemius Medialis is involved in the first synergy together with Soleus; this synergy represents the pre-swing phase, when plantar flexion occurs. To verify if any difference between synergies weights exists Cosine similarity has been calculated.

Synergy	CS prox-SENIAM	CS prox-dist	CS dist-SENIAM
Synergy 1	**0.9998**	**1**	**0.9999**
Synergy 2	**0.9999**	**0.9997**	**0.9992**
Synergy 3	**0.9999**	**0.9999**	**1**
Synergy 4	**1**	**1**	**1**

Table 5.2: Cosine similarity calculated from synergy weights obtained changing electrode positioning along GM of Subject 1. All CS value are above 0.90.

As shown by Table 5.2 all Cosine Similarity values are above 0.9, this means that there isn't difference between synergies extracted moving the electrodes along Gastrocnemius Medialis.

5.2 Muscle synergy extraction results during cycling

Muscle synergy extraction was performed for cycling as well. Three muscle synergies were obtained for all subjects. The same three subjects excluded from gait analysis are not taken in account again due to the artefacts corrupting EMG signals.

5.2.1 Muscle synergy extraction changing electrode positioning along Rectus Femoris

In this section the results about differences in EMG detected from the proximal, SENIAM, and distal electrode positioning on the Rectus Femoris muscle are reported. The EMG signals for all other muscles (included Gastrocnemius medialis) are from the SENIAM positioning. Envelopes calculated from different electrode location along Rectus Femoris showed that 3 subjects out of 5 have a localized activation of proximal portion of the muscle during hip flexion during initial upstroke phase, and distal region during knee extension at downstroke phase. It must be pointed out that even if this behaviour is shown in more than one subject it is not always well defined, only one subject clearly shows a different activation between proximal and distal region.

Since only one subject has clearly shown a non-uniformly activation of Rectus Femoris the results of two representative subjects are reported in the following.
Figures 5.10 and 5.11 shows the envelopes normalized in time and amplitude of ten gait cycles. For Subject 1 (fig. 5.10) EMG detected from the electrodes on the proximal RF region shows a clear activation during the hip flexion at upstroke phase (highlighted with red circle); this activation is lower moving to the central portion of the muscle, while it is absent for distal electrode positioning. Subject 5 (Fig. 5.10) does not show any difference between different electrode placements.

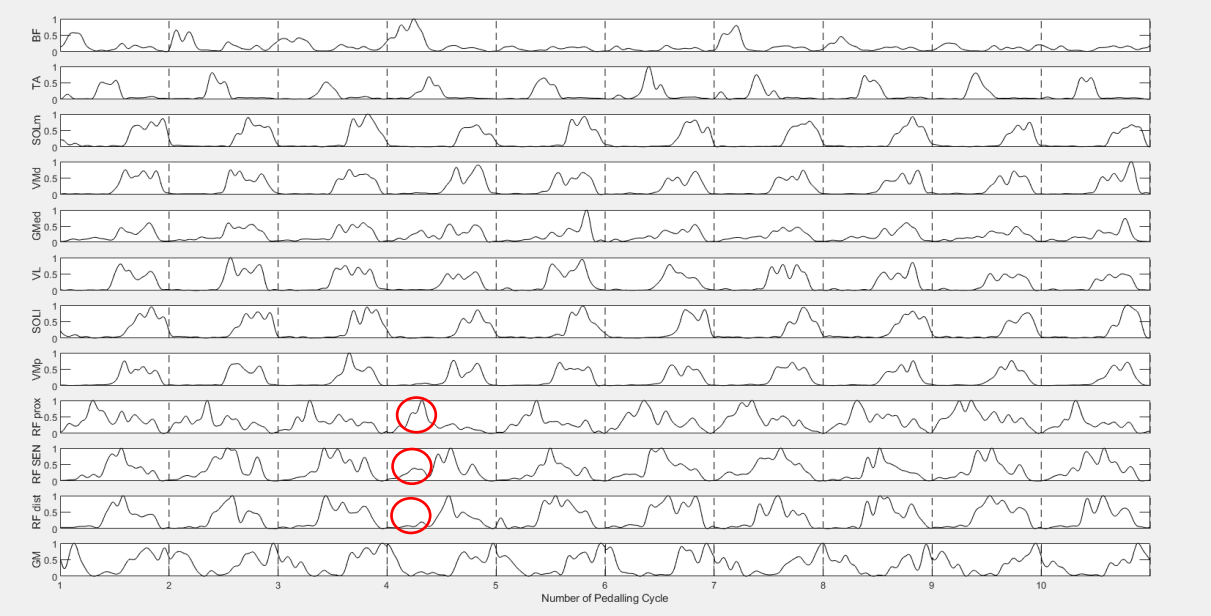

Figure 5.10: EMG envelopes for all muscles during ten pedalling cycles for Subject 1. The length of each gait cycle is normalized to 200 samples. The envelope for each muscle is normalized in amplitude with respect to the maximum of the envelope. On the x-axis the number of each pedalling cycle is reported. Red circles indicates the activation of RF during hip flexion, this activation can't be appreciated when electrodes are placed in proximal and SENIAM position, it is absent for distal position.

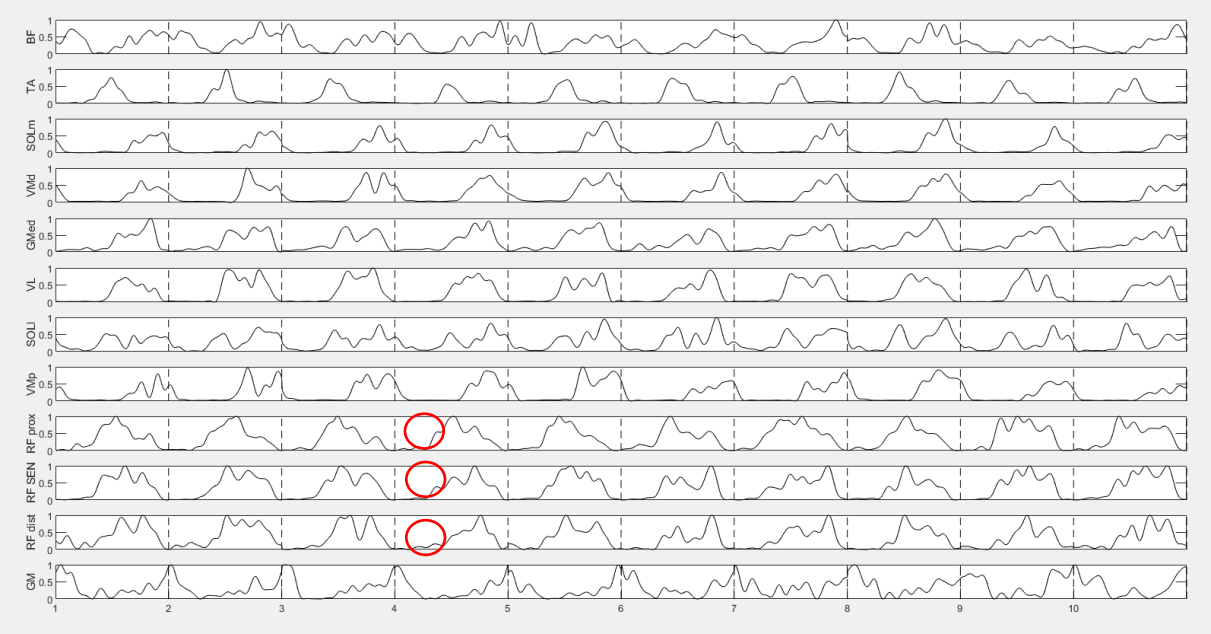

Figure 5.11: EMG envelopes for all muscles during ten pedalling cycles for Subject 5. The length of each gait cycle is normalized to 200 samples. The envelope for each muscle is normalized in amplitude with respect to the maximum of the envelope. On the x-axis the number of each pedalling cycle is reported. Red circles indicates the activation of RF during hip flexion, in this case it is absent as highlighted by red circles.

Muscle synergy extraction was performed using the mean envelope estimated on ten gait cycles. Figures 5.12 and 5.13 show the average envelopes for Subject 1 and 5.

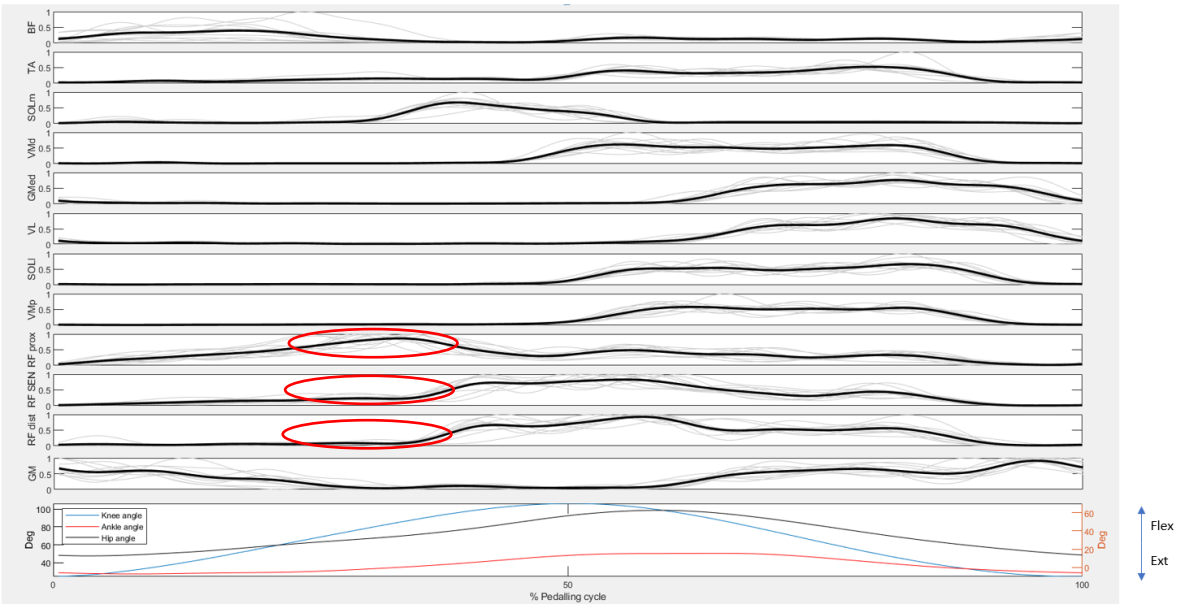

Figure 5.12: All cycle for each muscle of Subject 1 is overlapped and the mean calculated (thick black line). the mean behaviour of knee (blue), ankle (red) and hip (black) angles are reported. The activation is evident for proximal electrode positioning only as highlighted (red circle).

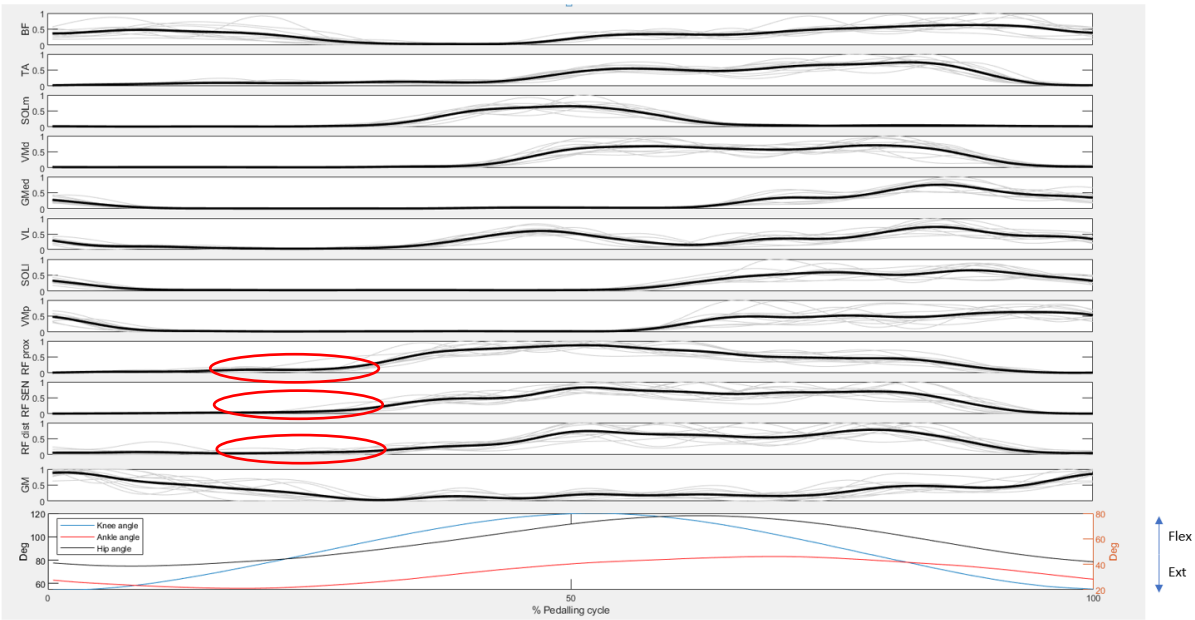

Figure 5.13: All cycle for each muscle of Subject 5 is overlapped and the mean calculated (thick black line). the mean behaviour of knee (blue), ankle (red) and hip (black) angles are reported. The activation is totally absent as highlighted (red circle).

In figures 5.14 and 5.615 RF mean envelopes, muscle synergy activation coefficients and weights and RF reconstructed envelopes for Subject 1 and 4 are shown.

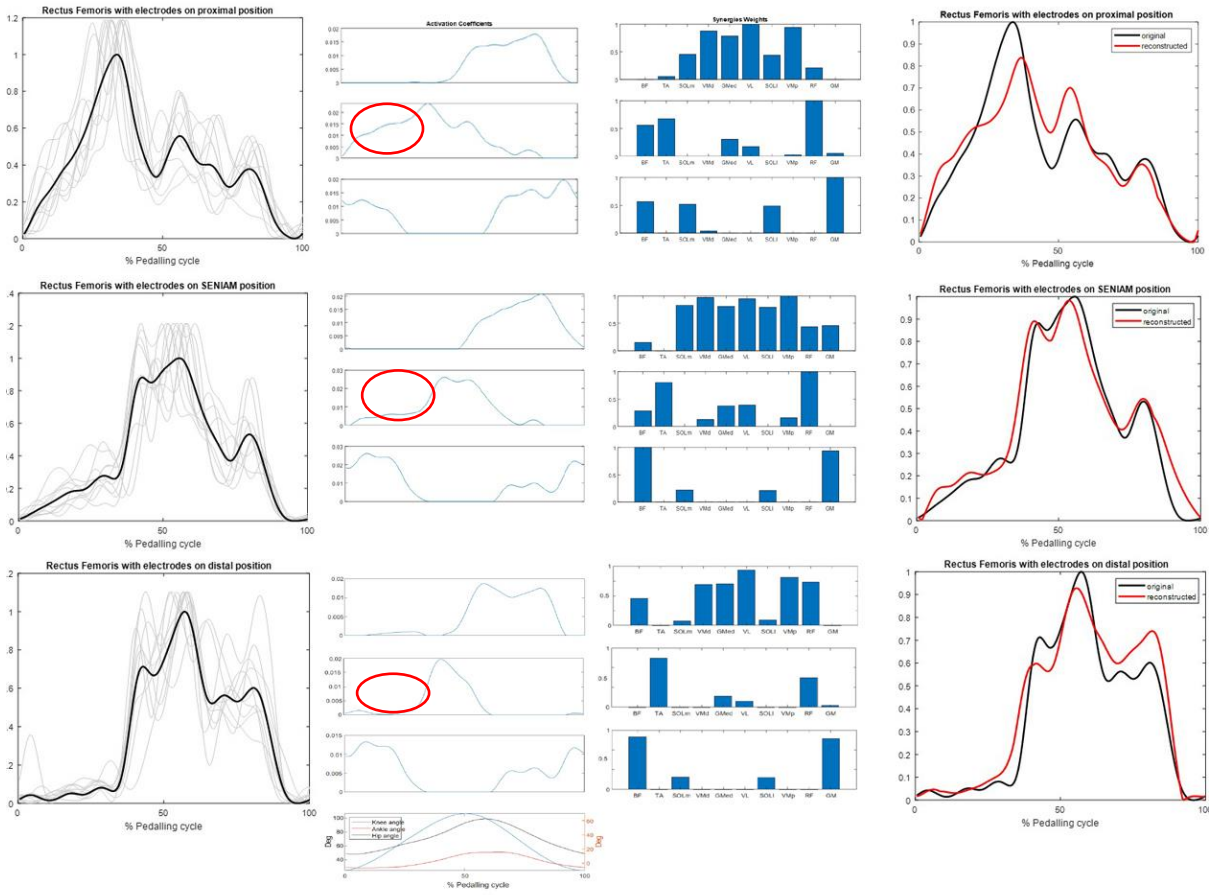

Figure 5.14: muscle synergy extraction results for Subject 1. Left column shows all RF overlapped envelopes and the average one (thick black line). central column shows the three extracted muscle synergies for the three different electrode positioning and joint angle graph. Right column shows average envelope and the reconstructed one, VAF of 0.90 provides a good quality of reconstruction. Synergy 2, that represent RF proximal activity, activation coefficient is characterized by a peak in correspondence of hip flexion for proximal electrode position, while it seems to disappear as concern SENIAM distal position. Synergy 3 represent the activity of RF during knee extension at downstroke phase, weight value Is higher for distal electrode positioning.

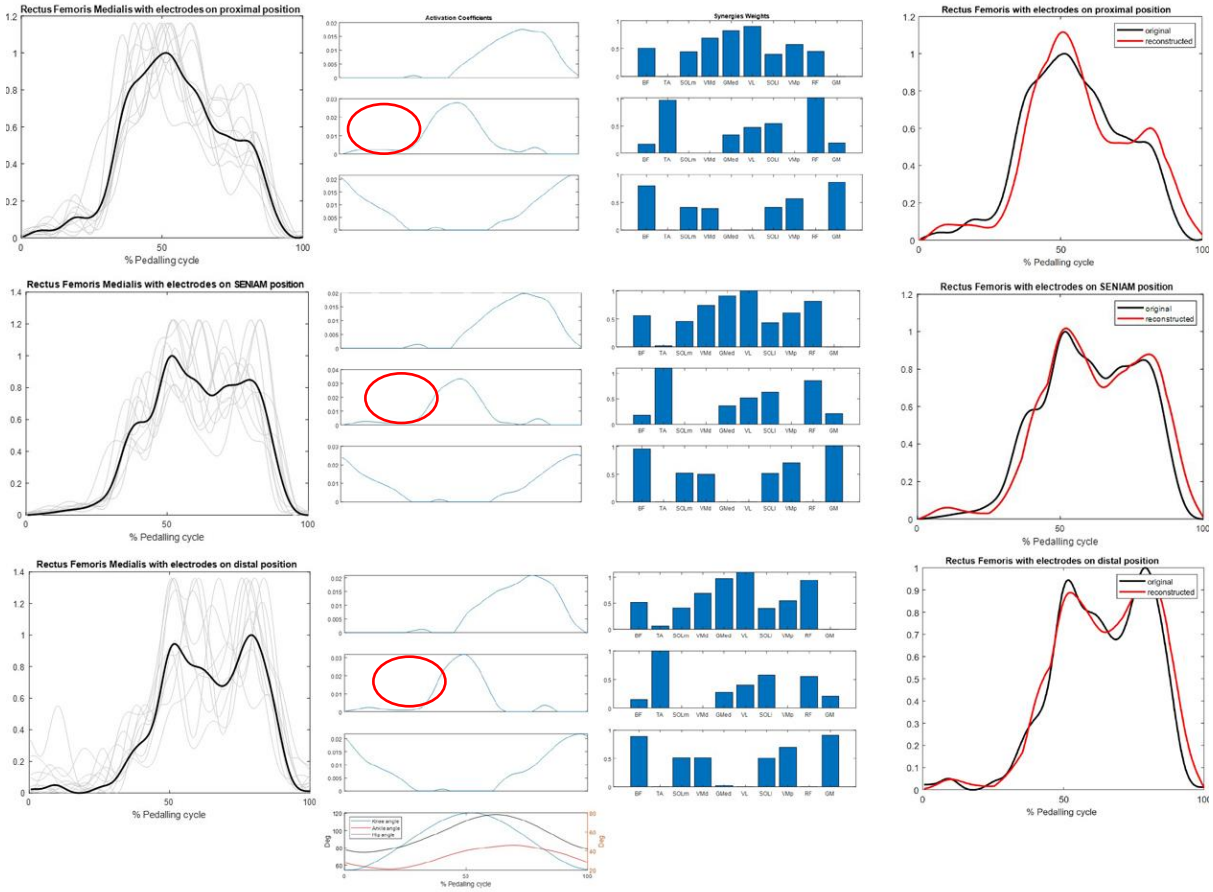

Figure 5.15: muscle synergy extraction results for Subject 5. Left column shows all RF overlapped envelopes and the average one (thick black line). central column shows the three extracted muscle synergies for the three different electrode positioning and joint angle graph. Right column shows average envelope and the reconstructed one, VAF of 0.90 provides a good quality of reconstruction. Synergy 2, that represent RF proximal activity, is absent. Synergy 3 represent the activity of RF during knee extension at downstroke phase, weight value Is higher for distal electrode positioning.

Comparing these results with previous studies in literature [17], the extracted muscle synergies during cycling show common behaviours: as described in Chapter 3.5, Synergy 1 from figure 5.14 describes the activity of Rectus Femoris, Gluteus Medius, Vastus Lateralis, Gastrocnemius Medialis, Vastus Medialis and Soleus during final upstroke phase and initial downstroke phase. Synergy 2 is represented by the activation of Tibialis Anterior, Rectus Femoris, Gluteus Medius and Soleus during upstroke phase of cycling. Synergy 3 is characterized by activation of Biceps Femoris, Semitendinosus, Gastrocnemius Medialis and Soleus during the upstroke phase.

Rectus Femoris is mainly represented by first and second synergies for Subject 1 and only by first synergy for Subject 5. As we can see from figures 5.14 moving the electrodes from proximal to distal region both weights and activation coefficients change. Both activation coefficients and weights change, mainly in second synergy that represent the upstroke phase, where hip flexion occurs . Subject 5 (fig. 5.15) doesn't show any different pattern activity during hip flexion, in fact both weights and coefficients don't seem to change moving the electrodes from Rectus Femoris' proximal to distal portions.

Cosine similarity is calculated to quantify the variation of synergy weights.

Synergy	Subject	CS prox-SENIAM	CS prox-dist	CS dist-SENIAM
Synergy 1	1	0.9510	0.7278	0.8808
	5	0.9876	0.9734	0.9959
Synergy 2	1	0.9558	0.7793	0.8810
	5	0.9910	0.9626	0.9896
Synergy 3	1	0.9058	0.9453	0.9614
	5	0.9995	0.9966	0.9987

Table 5.3: cosine similarity calculated from synergy weights obtained changing electrode positioning along RF. as highlighted in yellow synergy 1 and 2 of Subject 1 are the only ones with value of CS not above 0.90. Subject 5 does not show CS lower than 0.90.

As highlighted in yellow (Table 5.3) only Subject 1 shows Cosine similarity values not above 0.90. CS value for the second synergy is not above 0.90 comparing proximal and distal electrode positioning, this means that proximal is more involved than distal one, in fact this synergy represents the upstroke phase of pedalling cycling, while distal region seems to be more represented by first synergy, that characterizes downstroke phase, where knee flexion occurs. On the other hand, Subject 5 doesn't show any difference in synergy weights, as evidenced by Cosine similarity values.

5.2.2 Muscle synergy extraction changing electrode positioning along Gastrocnemius Medialis

In this section the results about differences in EMG detected from the proximal, SENIAM, and distal electrode positioning on the Gastrocnemius Medialis during cycling muscle are reported. The EMG signals for all other muscles (included Rectus Femoris) are from the SENIAM positioning. No subject showed a different activation of Gastrocnemius Medialis moving from proximal to distal region, for this reason muscle synergies from only one representative subject are reported. Figures 5.16 the envelopes normalized in time and amplitude of ten gait cycles for Subject 1.

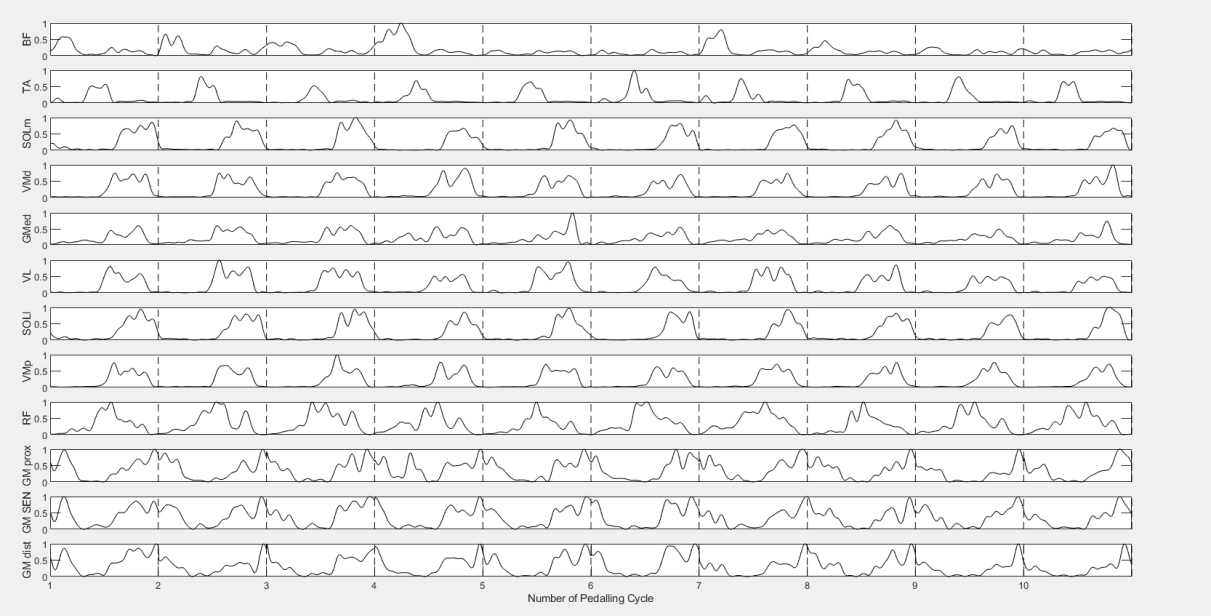

Figure 5.16: EMG envelopes for all muscles during ten pedalling cycles for Subject 1. The length of each gait cycle is normalized to 200 samples. The envelope for each muscle is normalized in amplitude with respect to the maximum of the envelope. On the x-axis the number of each pedalling cycle is reported. There is not evident difference in GM activation pattern.

Muscle synergy extraction was performed using the mean envelope estimated on ten gait cycles. Figure 5.17 shows the average envelopes for Subject 1.

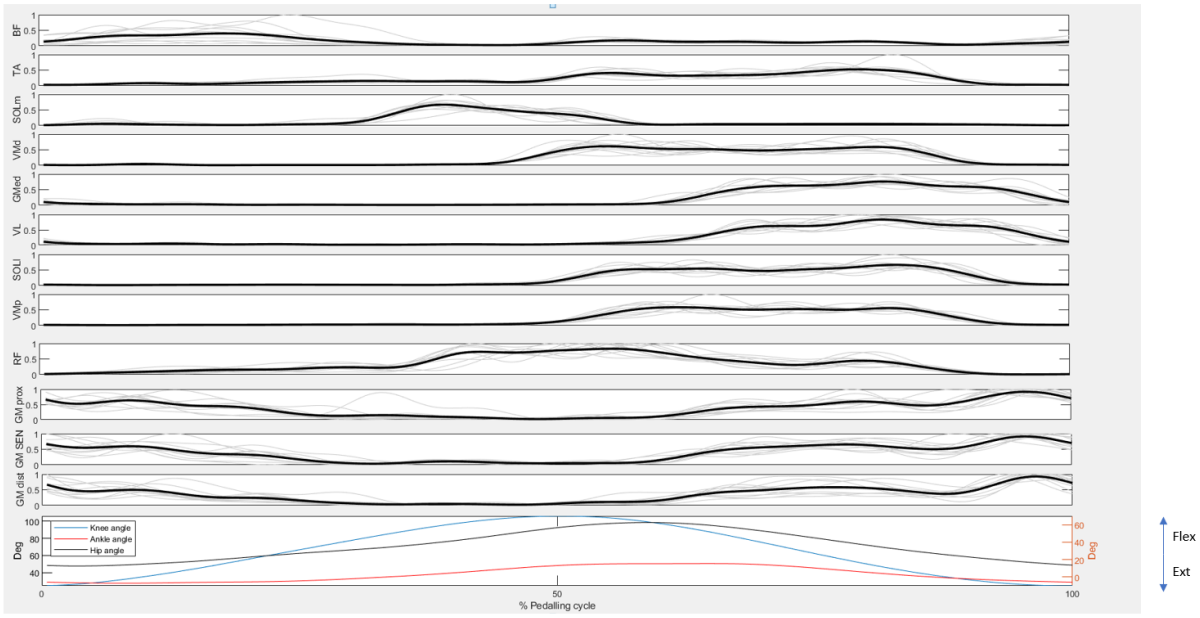

Figure 5.17: All cycle for each muscle of Subject 1 is overlapped and the mean calculated (thick black line). the mean behaviour of knee (blue), ankle (red) and hip (black) angles are reported. GM activation from different electrode positioning seems to be very similar.

In figures 5.18 GM mean envelopes, muscle synergy activation coefficients and weights and RF reconstructed envelopes for Subject 1 and 4 are shown.

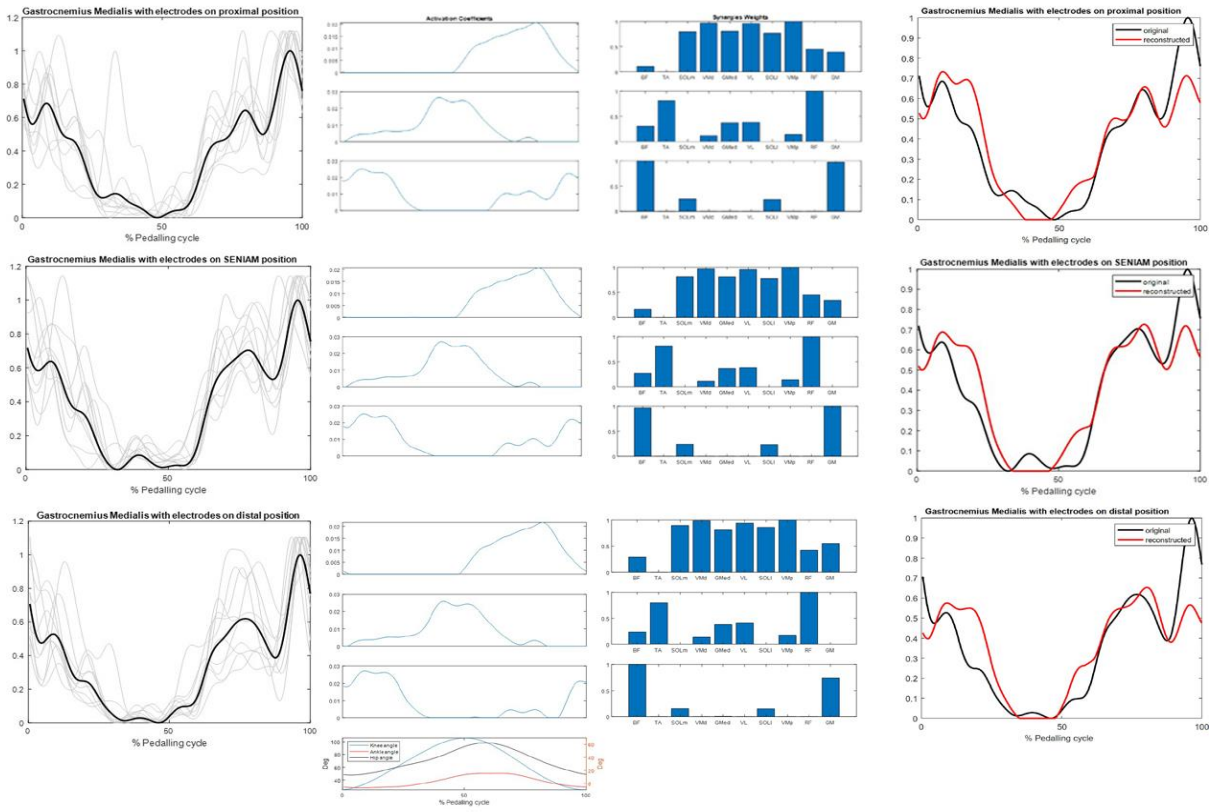

Figure 5.18: muscle synergy extraction results for Subject 1. Left column shows all GM overlapped envelopes and the average one (thick black line). central column shows the four extracted muscle synergies for the three different electrode positioning and joint angle graph. Right column shows average envelope and the reconstructed one, VAF of 0.90 provides a good quality of reconstruction. Synergy 1, that represent GM activity, activation coefficient and weights show little difference from proximal to distal electrode positioning.

Gastrocnemius Medialis is involved in the first synergy, that represents the downstroke phase, when plantar flexion occurs and third synergy and third synergy, corresponding to knee flexion during upstroke phase. To verify if any difference between synergies weights exists Cosine similarity has been calculated.

Synergies	CS prox-SENIAM	CS prox-dist	CS dist-SENIAM
Synergy 1	**0.9996**	**0.9847**	**0.9885**
Synergy 2	**0.9998**	**0.9989**	**0.9982**
Synergy 3	**0.9994**	**0.9940**	**0.9938**

Table 5.4: Cosine similarity calculated from synergy weights obtained changing electrode positioning along GM of Subject 1. All CS value are above 0.90.

As shown by Table 5.2 all Cosine Similarity values are above 0.9, this means that there isn't difference between synergies extracted moving the electrodes along Gastrocnemius Medialis.

6 Discussion

This study investigated the possible effect of different electrode positioning along bi-articular muscles on muscle synergy extraction. The main findings, as regards Rectus Femoris, are that no significant differences occur in muscle synergies during both tasks, because only one subject clearly shows a different activation from proximal to distal. Instead, Gastrocnemius Medialis activation patterns seem to be the same along the muscle length.

We started from the results obtained by Watanabe et al. [20][21][22] in their work, they find evidence of non-uniformly RF activation during gait and cycling. Envelopes calculated from RF EMG signals were comparable in only few cases with the ones calculated by them (Figures 6.1, 6.2, 6.3 and 6.4).

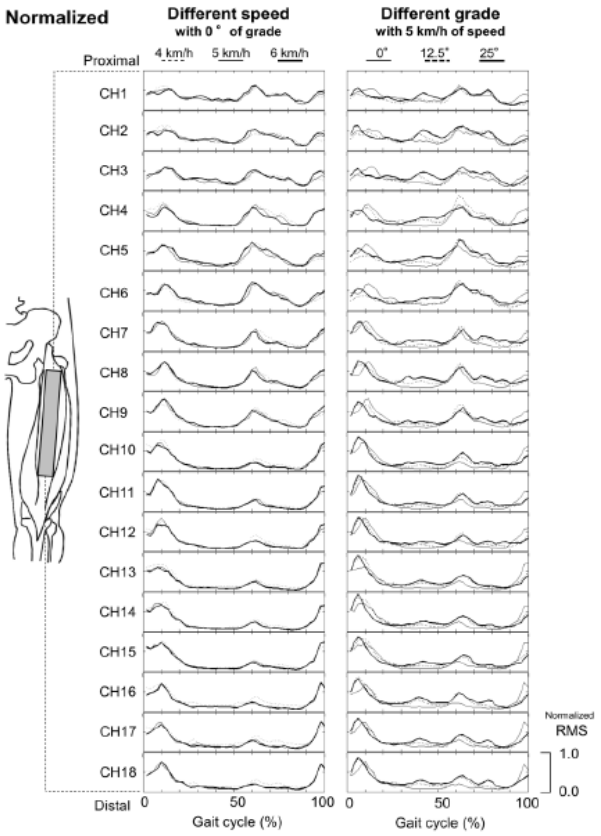

Figure 6.1: picture from Watanade et al. [20] – analysis of RF activity during gait on a treadmill: distal region seems to be more involved at the beginning and at the end of gait cycle, while proximal portion is more active during hip flexion, just before the beginning of swing phase.

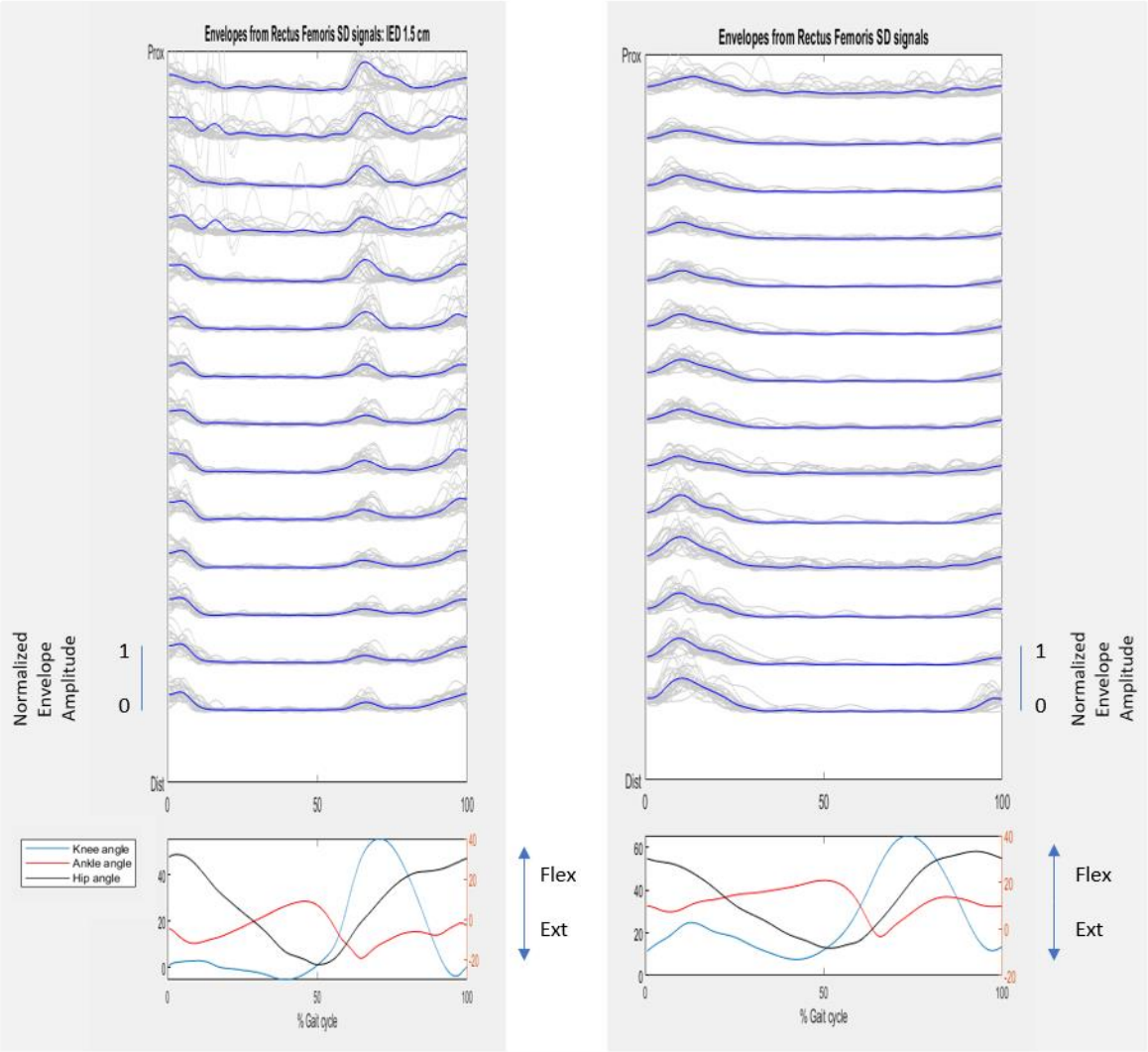

Figure 6.2: Rectus Femoris envelopes calculated from two different subject during gait. in one case (left) there is a clear activation of RF during hip flexion, this activity decreases from proximal to distal region. the other one (right) does not show any activity during pre-swing phase, only distal activity at the beginning and at the end of the cycle is evident.

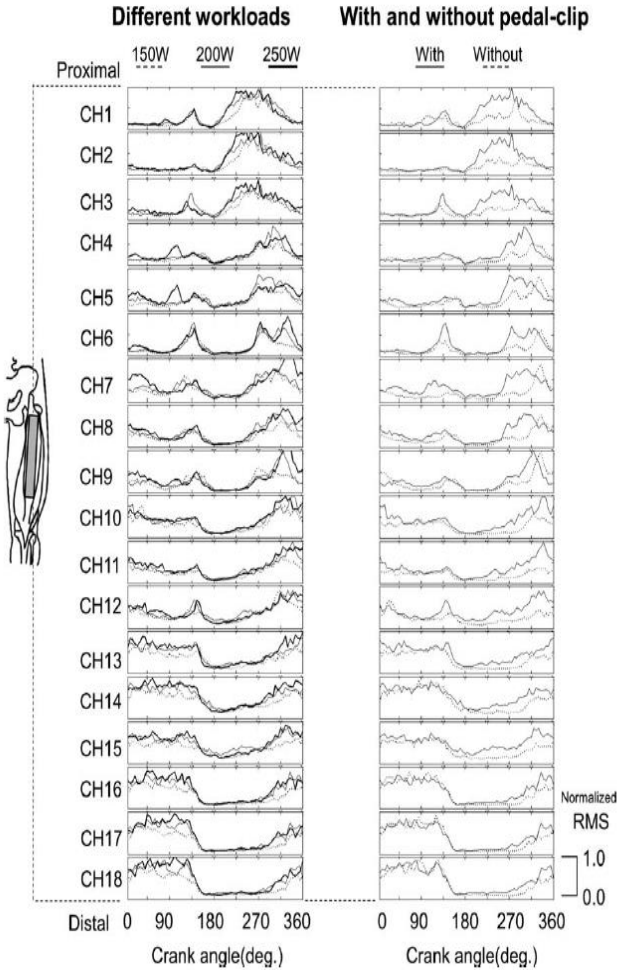

Figure 6.3: Watanabe et al. [22] analysis of Rectus Femoris regional-specific activation during cycling, proximal region is more involved during the first half of upstroke, when hip flexion occurs; distal portion is more active during downstroke, with knee extension.

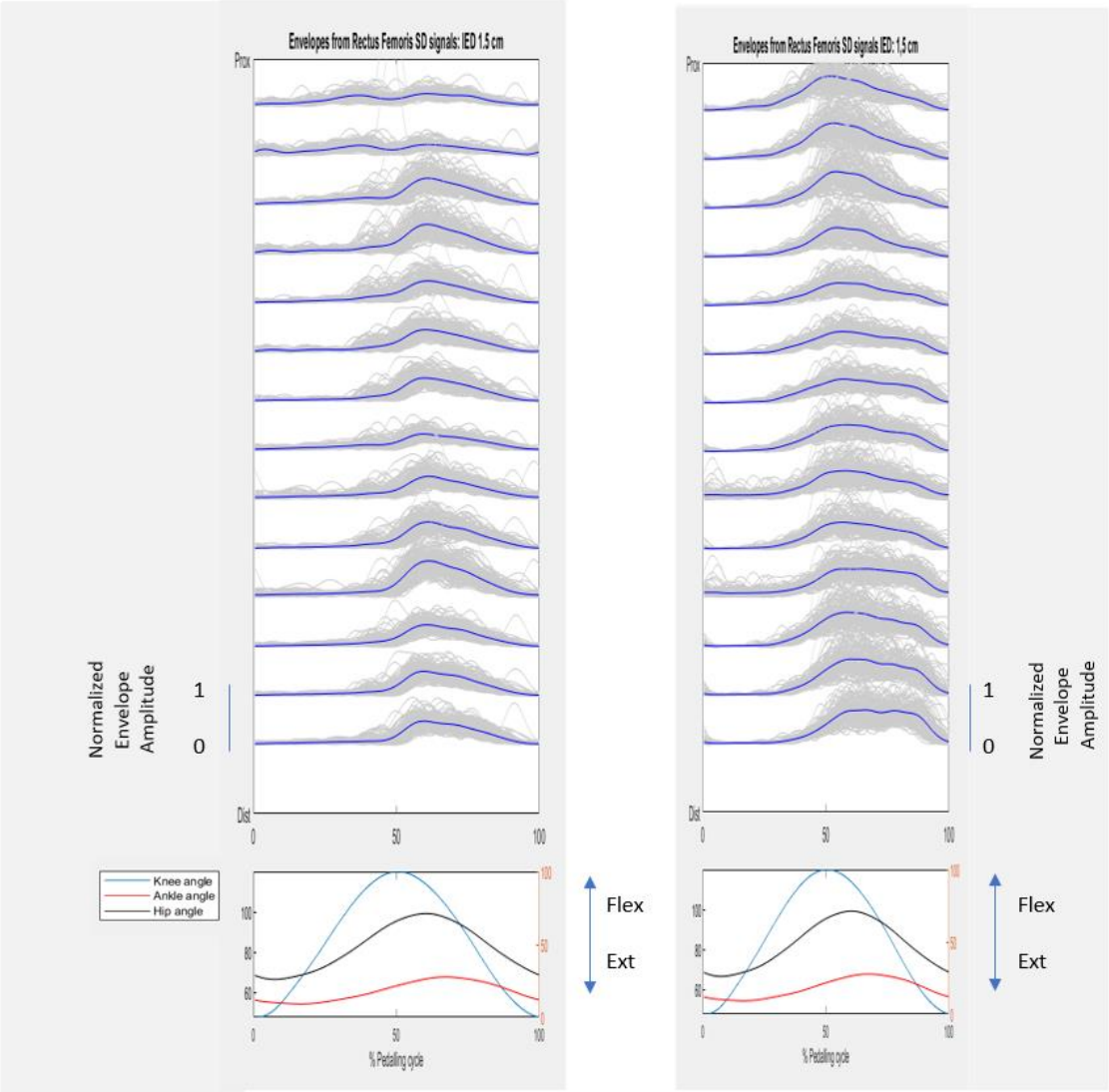

Figure 6.4: Rectus Femoris envelopes calculated from two different subject during cycling. in one case (left) there is an activation of RF during hip flexion, this activity decreases from proximal to distal region. the other one (right) does not show any activity during pre-swing phase, only distal activity at the beginning and at the end of the cycle is evident.

Figures 6.1, 6.2, 6.3 and 6.4 reveal the Rectus Femoris behaviour is comparable with the one found out by Watanabe in both walking and cycling. But this pattern is not common to all subjects, especially as regards gait. This could be due to different methodological approaches between this study and Watanabe et al. [20][22], in fact, in their work all subjects were instructed to perform walking on a treadmill at pre-selected speed, while in our experimental protocol it was decided to let subjects free to walk at their own pace. Lee SJ and Hidler J.[31] showed that some difference occurs between over-ground walking and treadmill walking in both biomechanics and muscle activity, for example during the transition from stance to swing the activity of Rectus Femoris is higher for treadmill walking.

Furthermore, it must be considered that the activation of proximal region of Rectus Femoris is more evident with high walking speed, in fact the lowest velocity set by Watanabe et al. is 4 km/h, the subjects that participate to this work walked at lower speed.

Another difference regards the electrode positioning. In their work [21] they determined it using ultrasonography, so they could identify the precise location of Rectus Femoris and the neighbour muscles. We identified the distal end of RF with palpation and the electrode matrix was attached following the line between iliac crest and patella, in this way we couldn't guarantee the same precision.

However, some subjects have shown a distinct activation between proximal and distal region of Rectus Femoris, which resulted in differences on muscle synergy. A limitation of this work is that muscle synergy extraction was performed using the average EMG signal, because concatenating cycles that belong to non-consecutive steps created discontinuities. The focus is to understand if a different electrode positioning can affect muscle synergies, so the average signals is a good choice as starting point, but with this approach the EMG variability is missed, so reconstruct the original signal from synergies extracted from average one results in low quality, and the details of signal will be lost. Best way to extract muscle synergies, with good quality of reconstruction, is to concatenate a high number of cycles (Oliveira et al. [30]).

Finally, a limited number of subjects were analysed, so increase the pool of subjects for further investigation is required to confirm the results of this work.

7 Conclusions

The aim of this study was to evaluate the possible effects of different electrode positioning along bi-articular muscles on muscle synergy extraction.

From different tests carried out, only one subject shown an interesting result, because Rectus Femoris was activated non-uniformly during both gait and cycling, this behaviour reflected on extracted muscle synergies. As regard Gastrocnemius Medialis there is no evidence of a distinct activation from proximal to distal region.

This result is promising for further investigation and evaluation. The recommendation is to increase the number of tested subjects and maintain the conditions similar to ones suggested by works that have investigated the selective activation within the same subject.

Appendix A – Informed Consent and Subject Form

Participant:_____

Date__/__ /___

Age: ____ years Heigth: ____ cm Body mass: ___ kg

Thigh Length		**Shank Length**	
left	right	left	right

Order	Task	Filename (Vicon)	Filename (bp)	Comments
	Walking at normal speed			
	Cycling at 60 rpm 150W no pedal-staps			

INFORMED CONSENT

This declaration refers to an experimental study that aims to assessing the effect of electrodes positioning on muscle synergies extraction.

Researcher:

Alice Chiara Moretti

Objective:

To extract muscle synergies, non-invasive EMG signals will be detected from some lower limb muscles, i.e.: Rectus Femoris, Gluteus Medius, Tibialis Anterior, Gastrocnemius Medialis, Soleus, Vastus Medialis, Vastus Lateralis, Biceps Femoris.
The main goal of this work is to assess if the electrode positioning produces some effects on muscle synergies extraction.

Experimental Session

Sixteen reflective markers will be placed with double-sided tape on pelvis, thigh, leg, and foot. Bipolar electrodes and electrodes matrix will be placed on the skin, that will be clean, scrubbed, and hairless.

Each subject will be required to perform 2 tests: a session of walking at normal speed, for 2 minutes with 2 minutes and a session of cycling at 60 rpm and 150W for 2 minutes.
The tests will be performed randomly. The entire duration of the experimental protocol is about 3 hours, and it will take place at Polito^{BIO}Med Lab (Biomedical Engineering Lab), Politecnico di Torino and it will be carried out by LISIN staff members.

Possible Risks:

The study is totally safe. At the end of the experiments the skin could be a little bit irritated after having removed the electrodes. The redness will disappear after a short time.

CONSENT REQUEST

I, the undersigned, _____ declare to be aware that:

- Every participant is free to ask for clarification about the experimental protocol.
- Any refusal to participate does not entail any consequences.
- The data collected shall not be disclosed in any event and will be processed anonymously.
- The results will be presented to avoid the identifiability of participants.

Also declare:

- To have carefully read the informed consent.
- To give the consent to participate in the study.

DATE: _____ SIGNATURE: _____

AUTHORIZATION FOR PERSONAL AND SENSITIVE DATA

I, the undersigned, _____

☐ CONSENT ☐ NOT CONSENT

the processing of personal and sensitive data collected in the context of this research in the terms and conditions indicated in the previous points. The processing of the data collected in the context of the research, their communication to third parties and/ or publication for scientific purposes are allowed but may only take place after the data have been anonymized, by and under the direct responsibility of the research manager. All researchers involved in the data collection are bound by the secrecy of the identity of the participants.

DATE: _____ SIGNATURE: _____

Bibliography

The EMG introductive chapter is based on:

***R. Merletti, P.A. Parker**, 2004. Electromyography: Phisiology, Engineering and Noninvasive Applications, IEEE Press, chapter 1.*

List of article and work consulted for the realization of the other chapters:

1. ***Bizzi E., Cheung VC.** (2013). The neural origin of muscle synergies. Frontiers in Computational Neuroscience. 7:51. 10.3389/fncom.2013.00051.*
2. ***Frère J., Hug F.** (2012). Between-subject variability of muscle synergies during a complex motor skill. Frontiers in Computational Neuroscience. 6:99. 10.3389/fncom.2012.00099.*
3. ***Saito A., Tomita A., Ando R., Watanabe K., Akima H.** (2018). Muscle synergies are consistent across level and uphill treadmill running. Scientific Reports. 13;8(1):5979. 10.1038/s41598-018-24332-z.*
4. ***Chvatal S. A., Ting L. H.** (2013). Common muscle synergies for balance and walking. Frontiers in Computational Neuroscience. 7:48. 10.3389/fncom.2013.00048.*
5. ***Wakeling JM, Horn T.** (2009) Neuromechanics of muscle synergies during cycling. J Neurophysiol. 101(2):843-54. 10.1152/jn.90679.2008. Epub 2008 Dec 10.*
6. ***Barroso F. O., Torricelli D., Molina-Rueda F., Alguacil-Diego I. M., Cano-de-la-Cuerda R., Santos C., Moreno J. C., Juan C. Miangolarra-Page, Pons J. L.** (2017). Combining muscle synergies and biomechanical analysis to assess gait in stroke patients. Journal of Biomechanics. 63 98-103. 10.1016/j.jbiomech.2017.08.006.*
7. ***Safavynia S., Torres-Oviedo G., Ting L.** (2011). Muscle synergies: implication for clinical evaluation and rehabilitation of movement. Top Spinal Cord Inj Rehabil . 17(1): 16-24. 10.1310/sci1701-16*
8. ***Ebied A., Kinney-Lang E., Spyrou L., Escudero J**. (2018). Evaluation of matrix factorisation approaches for muscle synergy extraction. Medical Engineering & Physics. 57 51-60. 10.1016/j.medengphy.2018.04.003.*
9. ***Alessandro C, Delis I, Nori F, Panzeri S, Berret B.** (2013). Muscle synergies in neuroscience and robotics: from input-space to task-space perspectives. Frontiers in Computational Neuroscience. 7:43. 10.3389/fncom.2013.00043.*
10. ***Rabbi M.F., Pizzolato C., Lloyd D.G., Carty C. P., Devaprakash D., Diamond L. E**. (2020). Non-negative matrix factorisation is the most appropriate method for extraction of muscle synergies in walking and running. Scientific Reports. 10:8266. 10.1038/s41598-020-65257-w.*

11. ***Tresch M. C., Cheung V. C. K., & D'Avella A.*** *(2006). Matrix factorization algorithms for the identification of muscle synergies: Evaluation on simulated and experimental data sets. Journal of neurophysiology. 95(4). 2199-221210.1152/jn.00222.2005.*
12. ***Lee D. D., Seung H. S.*** *(1999). Learning the parts of objects by non-negative matrix factorization. Nature. 401 788-791. 10.1038/44565*
13. ***Cappellini G, Ivanenko YP, Poppele RE, Lacquaniti F.*** *(2006). Motor patterns in human walking and running. J Neurophysiol. 95(6):3426-37.10.1152/jn.00081.2006. Epub 2006 Mar 22.*
14. ***Kim Y, Bulea TC, Damiano DL.*** *(2016). Novel Methods to Enhance Precision and Reliability in Muscle Synergy Identification during Walking. Front Hum Neurosci. 10:455. 10.3389/fnhum.2016.00455.*
15. ***Wojtara T, Alnajjar F, Shimoda S, Kimura H.*** *(2014). Muscle synergy stability and human balance maintenance. J Neuroeng Rehabil. 11:129.10.1186/1743-0003-11-129.*
16. ***Kibushi B, Hagio S, Moritani T, Kouzaki M.*** *(2018). Speed-Dependent Modulation of Muscle Activity Based on Muscle Synergies during Treadmill Walking. Front Hum Neurosci.12:4. 10.3389/fnhum.2018.00004.*
17. ***Barroso F. O., Torricelli D., Moreno J. C., Taylor J., Gomez-Soriano J., Bravo-Esteban E., Piazza S., Santos C., Pons J. L.*** *(2014). Shared muscle synergies in human walking and cycling. J Neurophysiol 112: 1984–1998. 10.1152/jn.00220.2014.*
18. ***Rimini D., Agostini V., Knaflitz M.*** *(2017). Evaluation of muscle synergies stability in human locomotion: A comparison between normal and fast walking speed. IEEE International Instrumentation and Measurement Technology Conference (I2MTC). pp. 1-5, 10.1109/I2MTC.2017.7969722.*
19. ***Hug F., Turpin N. A., Couturier A., Dorel S.*** *(2011) Consistency of muscle synergies during pedaling across different mechanical constraints. J Neurophysiol. 106(1):91-103. 10.1152/jn.01096.2010. Epub 2011 Apr 13.*
20. ***Watanabe K., Kouzaki M., Moritani T.*** *(2014) Regional neuromuscular regulation within human rectus femoris muscle during gait. J Biomech. 47(14):3502-8. 10.1016/j.jbiomech.2014.09.001. Epub 2014 Sep 16.*
21. ***Watanabe K., Kouzaki M., Moritani T.*** *(2012) Task-dependent spatial distribution of neural activation pattern in human rectus femoris muscle. J Electromyogr Kinesiol. 22(2):251-8. 10.1016/j.jelekin.2011.11.004. Epub 2011 Dec 5.*
22. *Watanabe K., Kouzaki M., Moritani T. (2015) Heterogeneous neuromuscular activation within human rectus femoris muscle during pedaling. Muscle Nerve. 52(3):404-11. 10.1002/mus.24544. Epub 2015 Jan 5.*
23. ***Hodson-Tole, E.F., Loram, I.D., & Vieira, T.M.*** *(2013). Myoelectric activity along human gastrocnemius medialis: Different spatial distributions of postural and electrically elicited surface potentials. Journal of Electromyography and Kinesiology, 23, 43 - 50. 10.1016/j.jelekin.2012.08.003.*

24. ***Watanabe K., Vieira T. M., Gallina A., Kouzaki M., Moritani T.*** *(2021) Novel Insights Into Biarticular Muscle Actions Gained From High-Density Electromyogram. Exerc Sport Sci Rev. 49(3):179-187. 10.1249/JES.0000000000000254.*
25. ***Cabral H. V., de Souza L. M., Mello R. G., Gallina A., de Oliveira L. F., Vieira T. M.****, (2018)**. Is the firing rate of motor units in different vastus medialis regions modulated similarly during isometric contractions? Muscle Nerve, 57: 279-286. 10.1002/mus.25688.*
26. ***Gallina A., Vieira T.*** *(2015). Territory and fiber orientation of vastus medialis motor units: A Surface electromyography investigation. Muscle Nerve, 52: 1057-1065. 10.1002/mus.24662.*
27. ***Staudenmann D., Kingma I., Daffertshofer A., Stegeman D. F., Van Dieën J. H. (****2009). Heterogeneity of muscle activation in relation to force direction: a multi-channel surface electromyography study on the triceps surae muscle. J. Electromyogr. Kinesiol. 19(5):882-95.. 10.1016/j.jelekin.2008.04.013.*
28. ***Kurz E., Faude O., Roth R. et al.*** *Ankle muscle activity modulation during single-leg stance differs between children, young adults and seniors. Eur J Appl Physiol 118**,** 239–247 (2018). 10.1007/s00421-017-3764-0.*
29. ***Cerone G. L., Botter A., Gazzoni M.*** *(2019). A Modular, Smart, and Wearable System for High Density sEMG Detection, IEEE Transactions on Biomedical Engineering. PP. 1-1. 10.1109/TBME.2019.2904398.*
30. ***Olivera A. S., Gizzi L., Farina D., Kersting U. G.*** *(2014). Motor modules of human locomotion: influence of EMG averaging, concatenation, and number of step cycles. Front. Hum. Neurosci. 8:335. 10.3389/fnhum.2014.00335.*
31. ***Lee S. J., Hidler J.*** *(2008) Biomechanics of overground vs. treadmill walking in healthy individuals. J Appl Physiol (1985). 104(3):747-55. 10.1152/japplphysiol.01380.2006. Epub 2007 Nov 29.*
32. ***Saitou K., Masuda T., Michikami D., Kojima R., Okada M. (****2001). Innervation zones of the upper and lower limb muscles estimated by using multichannel surface EMG. Journal of human ergology. 29. 35-52. 10.11183/jhe1972.29.35.*
33. ***d'Avella A., Bizzi E.****, (2005). Shared and specific muscle synergies in natural motor behaviors. Proc Natl. Acad. Sci USA 102: 3076–3081.*